

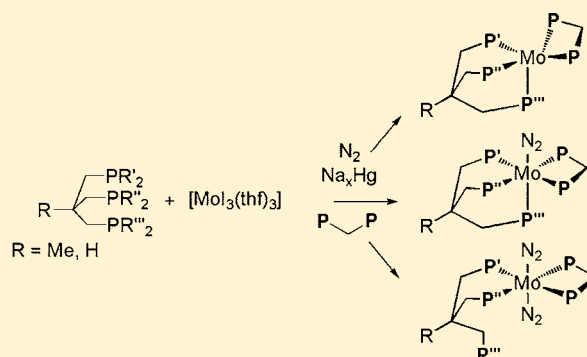
Bonding and Activation of N₂ in Mo(0) Complexes Supported by Hybrid Tripod Ligands with Mixed Dialkylphosphine/Diarylphosphine Donor Groups: Interplay of Steric and Electronic Factors

Ludger Sönksen, Christian Gradert, Jan Kraemer, Christian Näther, and Felix Tuzcek*

Institut für Anorganische Chemie, Christian Albrechts Universität Kiel, Max-Eyth-Strasse 2, D-24118 Kiel, Germany

S Supporting Information

ABSTRACT: Molybdenum dinitrogen complexes are presented which are supported by novel hybrid tripod ligands of the type Me-C(CH₂PPh₂)₂(CH₂PⁱPr₂) (**trpd-1**) and H-C(CH₂PPh₂)(CH₂PⁱPr₂)₂ (**trpd-2**) having mixed dialkylphosphine/diarylphosphine donor groups. Reaction of the ligand **trpd-1** with [MoI₃(thf)₃] followed by sodium amalgam reduction in the presence of the dppm gives the dinitrogen complex [Mo(N₂)(trpd-1)(dmpm)] where **trpd-1** is coordinated in a κ³ fashion. The complex exhibits a moderate activation of N₂ which enables its protonation under retention of the pentaphosphine ligation. Replacement of dmpm by the sterically more demanding coligand dppm is found to hamper coordination of N₂ and leads to [Mo(trpd-1)(dppm)], the first structurally characterized five-coordinate Mo(0) complex with a phosphine-only ligand sphere. Employing the ligand **trpd-2** along with the diphosphines dmpm and dppm in an analogous synthetic route results in a mixture of the bis(dinitrogen) complexes *trans*-[Mo(N₂)₂(κ²-trpd-2)(diphosphine)] and *trans*-[Mo(N₂)₂(*iso*-κ²-trpd-2)(diphosphine)] where the tripod ligand **trpd-2** coordinates with two phosphine arms and one phosphine group (PPh₂ or PⁱPr₂, respectively) is free. Similar results are obtained with the pure alkyl- and arylphosphine tripod ligands H-C(CH₂PⁱPr₂)₃ (**trpd-3**) and H-C(CH₂PPh₂)₃ (**tdppmm**), leading to *trans*-[Mo(N₂)₂(κ²-trpd-3)(diphos)] and *trans*-[Mo(N₂)₂(κ²-tdppmm)(dmpm)], respectively. The electronic and steric reasons for the experimental findings are considered, and the implications of the results for the area of synthetic nitrogen fixation with molybdenum phosphine systems are discussed.



INTRODUCTION

Coordination and activation of the highly inert, nonpolar molecule dinitrogen to enable its reduction to ammonia or its functionalization to high-value nitrogen-containing compounds are topics of fundamental interest in inorganic and organometallic chemistry.^{1–6} Synthetic nitrogen fixation in particular refers to the conversion of dinitrogen to ammonia in homogeneous solution and under ambient conditions.⁷ The first complete mechanistic scenario for this reaction was the Chatt cycle which starts by protonation of bis(dinitrogen) phosphine-Mo/W complexes carrying diphosphine ligands like dpe or depe.⁸ Our group has been involved in synthetic, spectroscopic, and theoretical investigations of Chatt type complexes over the past years.^{9–21} The classic Chatt cycle, however, suffers from a couple of drawbacks that limit its performance in a catalytic reaction mode. In particular, the conjugate base of the acid applied for protonation displaces one of the dinitrogen ligands in the parent bis(dinitrogen) complex, leading to a loss of 50% of bound substrate. Moreover, the presence of anionic coligands causes disproportionation at the Mo^I stage which corresponds to 50% loss of reactive complex.²²

One possible strategy to avoid these problems is to occupy the position *trans* to the dinitrogen ligand in the Mo⁰ complex by a phosphine group. To achieve this goal tridentate phosphine ligands like dpepp (bis(diphenylphosphinoethyl)-phenylphosphine) have already been applied, leading to complexes of the type [Mo(N₂)(dpepp)(diphosphine)] (diphosphine = dppm (bis(diphenylphosphino)methane), dmpm (bis(dimethylphosphino)methane), dpe (1,2-bis(dimethylphosphino)ethane), depe (1,2-bis(ethylphosphino)ethane), and 1,2-dppp (R-(+)-1,2-bis(diphenylphosphino)propane)).^{23–27} Because of the linear topology of the dpepp ligand, however, different isomeric forms of the mentioned complexes with varying degrees of activation exhibited by the dinitrogen ligand were obtained.^{23,27} As we have shown recently, this complication can be avoided by use of tridentate, symmetric tripod phosphine ligands like 1,1,1-tris(diphenylphosphinomethyl)ethane (tdppme) along with bidentate coligands like dmpm or dppm, leading to complexes of the type [Mo(N₂)(tdppme)(diphosphine)].²⁸ The tripod

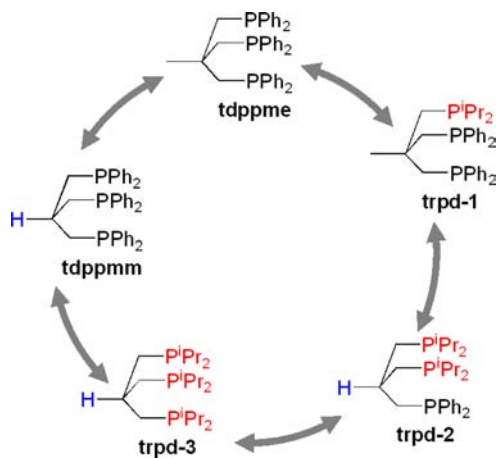
Received: March 8, 2013

Published: May 22, 2013

geometry of the ligand *tdppme* was in fact found to enforce the desired facial coordination, and formation of isomeric complexes was eliminated.

The complex $[\text{Mo}(\text{N}_2)(\text{tdppme})(\text{dppm})]$ exhibited a weak activation of N_2 . By choosing *dmpm* as coligand, however, the activation of the dinitrogen ligand could be increased significantly, allowing its protonation to $[\text{Mo}(\text{NNH}_2)(\text{tdppme})(\text{dmpm})](\text{OTf})_2$. This was ascribed to the fact that alkyl phosphine donor groups provide more electron density to the metal center for the activation of dinitrogen than their arylphosphine counterparts.²⁸ Replacement of aryl- by alkylphosphine donor groups within the tripod ligand *tdppme* would, of course, have a similar effect. Moreover, it would principally allow examining the variation of the substituents at the phosphine group in the *trans*-position to the N_2 ligand, which is not possible with the equatorially coordinating, bidentate coligands *dppm* and *dmpm*. We therefore wanted to prepare a set of tripod ligands in which the diphenylphosphine groups are replaced by diisopropylphosphine groups in a stepwise fashion, anticipating that in one of the resulting molybdenum dinitrogen complexes one of these groups would be positioned *trans* to the N_2 ligand. Following this idea, the new ligands **trpd-1** ($\text{Me}-\text{C}(\text{CH}_2\text{PPh}_2)_2(\text{CH}_2\text{P}^i\text{Pr}_2)$) with one diisopropylphosphine group, **trpd-2** ($\text{H}-\text{C}(\text{CH}_2\text{PPh}_2)(\text{CH}_2\text{P}^i\text{Pr}_2)_2$) with two and **trpd-3** ($\text{H}-\text{C}(\text{CH}_2\text{P}^i\text{Pr}_2)_3$) with three diisopropylphosphine groups were synthesized (Scheme 1). For preparative reasons the methyl group on the apical

Scheme 1



atom of the tripod was replaced by a hydrogen atom in the ligands **trpd-2** and **trpd-3**, leading to an isobutyl backbone in these systems. To allow a direct comparison between the two different tripod architectures the isobutyl version of *tdppme*, that is, the symmetric arylphosphine tripod 1,1,1-tris(diphenylphosphinomethyl)methane ($\text{H}-\text{C}(\text{CH}_2\text{PPh}_2)_3$; **tdppmm**),²⁹ has been included in this study as well (Scheme 1; double arrows denote substitutions of one group at the phosphine donors or at the backbone atoms).

In the present study this set of tripod ligands is employed in combination with the diphosphine coligands *dmpm* and *dppm* to the synthesis of molybdenum dinitrogen complexes. The resulting compounds are characterized by X-ray crystallography as well as vibrational and NMR spectroscopy, and their reactivity with respect to protonation is investigated. The implications of the results for the area of synthetic nitrogen fixation with molybdenum phosphine complexes are discussed.

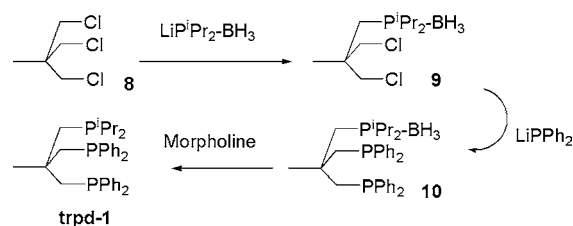
RESULTS AND ANALYSIS

1. Synthesis and Constitution of the Complexes.

A. Ligand Synthesis. To prepare ligands **trpd-1** and **trpd-2** with mixed diisopropyl-/diphenylphosphine end groups a preparative method was applied that is based on mono- or disubstituted proligands obtained by stoichiometric addition of the respective lithium phosphide to the respective trichloro precursor.³⁰

$\text{Me}-\text{C}(\text{CH}_2\text{PPh}_2)_2(\text{CH}_2\text{P}^i\text{Pr}_2)$ (**trpd-1**). The reaction route starts with substitution of one chlorine group of 1,1,1-tris(chloromethyl)ethane (**8**) by borane-protected lithium diisopropyl phosphide $\text{LiP}^i\text{Pr}_2-\text{BH}_3$, giving 1,1-(bis(chloromethyl))-1-(diisopropylphosphinoboranemethyl)ethane, $\text{Me}-\text{C}(\text{CH}_2\text{Cl})_2(\text{CH}_2\text{P}^i\text{Pr}_2-\text{BH}_3)$ (**9**; Scheme 2).

Scheme 2



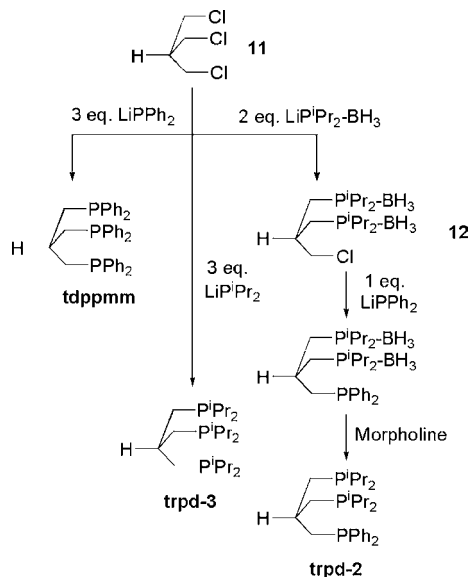
Addition of 2 equiv of lithium diphenyl phosphide results in compound **10**, and subsequent deprotection by morpholine leads to the mixed diisopropyl-/diphenylphosphine tripod 1,1-(bis(diisopropylphosphinomethyl))-1-(diphenylphosphinomethyl)ethane, $\text{Me}-\text{C}(\text{CH}_2\text{PPh}_2)_2(\text{CH}_2\text{P}^i\text{Pr}_2)$ (**trpd-1**).

The synthesis of mixed alkyl aryl tripod ligands on this route is limited by two factors, the large steric demand of borane-protected diisopropyl phosphide and the little space being available in the neopentyl backbone. Use of the borane protection group, on the other hand, is required for the purification procedures by column chromatography. The described problem is illustrated by the fact that addition of 2 equiv of $\text{Li}-\text{P}^i\text{Pr}_2-\text{BH}_3$ to **8** primarily results in $\text{Me}-\text{C}(\text{CH}_2\text{Cl})_2(\text{CH}_2\text{P}^i\text{Pr}_2-\text{BH}_3)$ (**9**) as well. Consequently, it was not possible to introduce two of the borane-protected diisopropyl phosphine groups into the neopentyl backbone.

$\text{H}-\text{C}(\text{CH}_2\text{PPh}_2)(\text{CH}_2\text{P}^i\text{Pr}_2)_2$ (**trpd-2**). To substitute two chlorine groups of the tris(chloromethyl) precursor by borane-protected lithium diisopropylphosphide we had to switch to a tripod with an isobutyl backbone (Scheme 3). We expected that because of the absence of the central methyl group the precursor 1,1,1-tris(chloromethyl)methane (**11**) should exhibit a significantly lower steric hindrance regarding substitution of the chlorine atoms. In fact, addition of 2 equiv of $\text{LiP}^i\text{Pr}_2-\text{BH}_3$ to **11** led to doubly borane-protected 1-(chloromethyl)-1,1-bis(diisopropylphosphinomethyl)methane (**12**) (Scheme 3, right). Subsequent substitution of the remaining chlorine atom by LiPPh_2 and deprotection in morpholine afforded 1,1-bis(diisopropylphosphinomethyl)-1-(diphenylphosphinomethyl)methane, $\text{H}-\text{C}(\text{CH}_2\text{PPh}_2)(\text{CH}_2\text{P}^i\text{Pr}_2)_2$ (**trpd-2**), which exhibits an inverted distribution of phosphine donor groups as compared to **trpd-1**.

$\text{H}-\text{C}(\text{CH}_2\text{P}^i\text{Pr}_2)_3$ (**trpd-3**) and $\text{H}-\text{C}(\text{CH}_2\text{PPh}_2)_3$ (**tdppmm**). Addition of 3 equiv of LiP^iPr_2 or LiPPh_2 to **11** (Scheme 3, middle, left) gave the respective symmetric tripod ligands 1,1,1-tris(diisopropylphosphinomethyl)methane (**trpd-3**) and 1,1,1-tris(diphenylphosphinomethyl)methane (**tdppmm**), respec-

Scheme 3



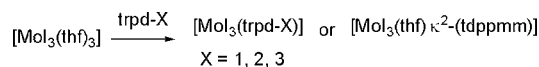
tively. The ligand **trpd-3** is the first tripodal ligand with three diisopropylphosphine end groups on the basis of a carbon backbone. The tripod **tdppmm** has already been synthesized by Janssen et al.²⁹

B. Synthesis and Constitution of Mo(III) and Mo(0) Complexes. Molybdenum dinitrogen complexes with the set of tripod ligands described above were prepared employing the Mo(III) precursors $[\text{MoX}_3(\text{tripod})]$ $X = \text{Cl, Br, I}$, which in turn can be synthesized by reacting $[\text{MoX}_3(\text{thf})_3]$ with the respective tripod ligand in THF or toluene.^{28,31–33} Subsequent sodium amalgam reduction under a nitrogen atmosphere with addition of the respective diphosphine coligand then afforded the corresponding dinitrogen complex.

Mo(III) Complexes. Because of facile substitution of the three tetrahydrofuran (thf, THF) ligands, the Mo(III) precursors $[\text{MoX}_3(\text{thf})_3]$ ($X = \text{Cl, Br, I}$) are well suited for the coordination of tridentate ligands.³⁴ A barrier for the coordination of tripod ligands lies in the fact that the thf ligands in all $[\text{MoX}_3(\text{thf})_3]$ complexes are coordinated in meridional geometry,^{35–37} which has to change to facial in the target compounds. For $[\text{MoI}_3(\text{thf})_3]$ such a change has, for example, been observed in the conversion to *fac*- $[\text{MoI}_3(\text{dppe})(\text{PMe}_3)]$.³² The reactions of $[\text{MoBr}_3(\text{thf})_3]$ and $[\text{MoCl}_3(\text{thf})_3]$ with **tdppme** provided further evidence for the transition from a meridional to a facial coordination^{28,33} However, refluxing a solution of the tripod ligand **trpd-1** in toluene with $[\text{MoBr}_3(\text{thf})_3]$, as successfully applied for the coordination of the **tdppme** ligand to Mo(III),²⁸ turned out to be too harsh for our mixed dialkylphosphine/diarylphosphine tripods. Only low quantities of product could be obtained which in addition were contaminated by black impurities, probably because of a possible oxidation of the alkyl phosphines. Similar degradation reactions have been observed upon refluxing $[\text{MoI}_3(\text{PET}_3)_3]$ and $[\text{MoCl}_3(\text{PMe}_3)_3]$ in toluene.³⁶ More gentle reaction conditions, that is, stirring at ambient temperature in THF, which successfully have been applied by Dahlenburg et al. to the coordination of linear multidentate alkylphosphane ligands to $[\text{MoCl}_3(\text{thf})_3]$,³¹ gave unsatisfyingly low yields, too. Replacement of the solvent THF by a mixture of THF and dichloromethane neither lead to improvements regarding the yield and the purity of the products.³³

It turned out that the best results for the ligands employed in this study are obtained by stirring $[\text{MoI}_3(\text{thf})_3]$ ^{32,38} with the respective tripod overnight at room temperature in THF (Scheme 4). The resulting red solution was concentrated, and

Scheme 4



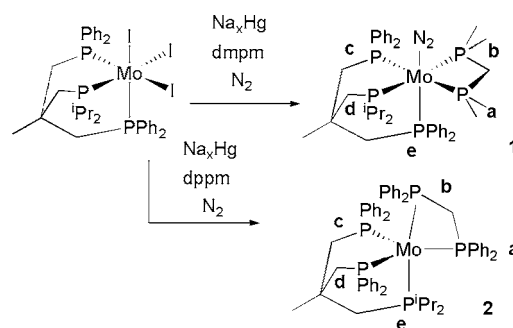
the $[\text{MoI}_3(\text{trpd-X})]$ complex was isolated after precipitation upon addition of diethyl ether or hexane. The tripod complexation occurs reasonably fast and can be performed in a practical time range. Furthermore, the synthesis is generally applicable and allows the preparation of the different molybdenum(III) tripod complexes in good purities and high yields.

After the subsequent sodium amalgam reduction (see below) the ligands **trpd-X** ($X = 2, 3$) and **tdppmm** are found to be coordinated in a κ^2 -fashion. This raises the question about the coordination mode on the Mo(III) stage. Elemental analysis and DTA-TG measurements show no evidence for remaining coordinated thf ligands in the Mo(III) complexes with the neopentyl ligand **trpd-1** and the isobutyl ligands **trpd-2** and **trpd-3** (Supporting Information, Figures S1–S3). In contrast, the Mo(III) complex with isobutyl tripod **tdppmm** seems to be coordinated in a κ^2 -fashion, corresponding to the complex $[\text{MoI}_3(\text{thf})\kappa^2\text{-(tdppmm)}]$. This is indicated by the fact that the DTA-TG measurement shows a mass loss at 137 °C that corresponds to one coordinated thf-ligand (–6%, MID 72 *m/z*) (Supporting Information, Figure S4).

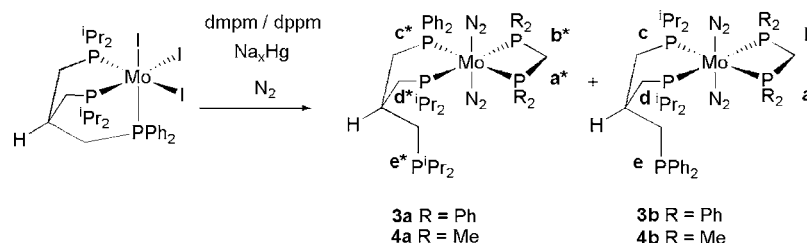
Mo(0) Dinitrogen Complexes. To obtain molybdenum dinitrogen complexes supported by our mixed tripod ligands, the respective precursor was stirred with sodium amalgam (7–11 equiv) in THF under a nitrogen atmosphere with addition of 1 equiv of **dmpm** or **dppm** as coligands. After partial evaporation of the solvent THF, addition of methanol and further concentration of the solution, the dinitrogen complexes could be obtained as red precipitates or red viscous oils, depending on the tripod ligand and the employed coligand.

$[\text{Mo}(\text{N}_2)(\text{trpd-1})(\text{dmpm})]$ (1). Reduction of $[\text{MoI}_3(\text{trpd-1})]$ with **dmpm** resulted in the octahedral Mo(0) pentaphosphine complex $[\text{Mo}(\text{N}_2)(\text{trpd-1})(\text{dmpm})]$ (**1**; Scheme 5). As inferred from X-ray structure analysis and ³¹P NMR spectroscopy (see below), the diisopropyl phosphine group is coordinated in the equatorial plane of this complex, in *cis* position to the axial dinitrogen ligand. The other possible coordination isomer with the diisopropyl phosphine group in *trans* position to the N_2 ligand is not formed.

Scheme 5



Scheme 6



$[\text{Mo}(\text{trpd-1})(\text{dppm})]$ (**2**). Reduction of $[\text{MoI}_3(\text{trpd-1})]$ in the presence of dppm did not lead to a dinitrogen complex. The reaction instead resulted in a red powder which according to elemental analysis and vibrational spectroscopy does not contain dinitrogen. This result was supported by ^{31}P NMR spectroscopy (see below) which indicates that $[\text{Mo}(\text{trpd-1})(\text{dppm})]$ (**2**) is a Mo(0) complex that contains only five coordinated phosphine groups (Scheme 5). As for the related complexes $[\text{Mo}(\text{N}_2)(\text{tdppme})(\text{dmpm})]$ and $[\text{Mo}(\text{N}_2)(\text{trpd-1})(\text{dmpm})]$ (vide supra) conventional octahedral coordination geometries have been evidenced, this rare coordination mode obviously results from replacement of one PPh_2 by a sterically more demanding P^iPr_2 group in the tdppme ligand along with replacement of dmpm by the bigger coligand dppm.

Possible limiting geometries for complex **2** are square-pyramidal or trigonal-bipyramidal. The latter has been observed for the five coordinate complex $[\text{Mo}(\text{C}_2\text{H}_2)(\text{dppe})_2]$ by Ishino et al.³⁹ A trigonal-bipyramidal structure is also indicated by the crystal structure analysis of **2** (see below). The ^{31}P NMR spectrum of **2**, however, is not compatible with this geometry and rather indicates a trigonal-pyramidal structure with the dppm ligand rotating around an axis that is approximately perpendicular to the plane of the three tripod P atoms. To the best of our knowledge, no other structurally characterized example for such a five-coordinate Mo(0) complex exists in the literature.

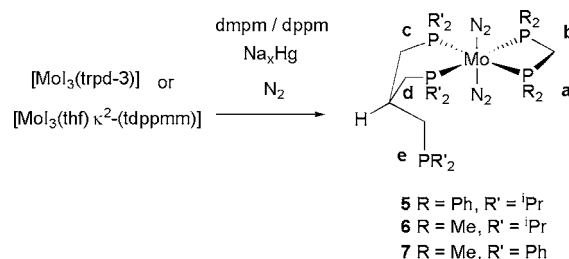
$[\text{Mo}(\text{N}_2)_2(\kappa^2\text{-trpd-2})(\text{dppm})]/[\text{Mo}(\text{N}_2)_2(\text{iso-}\kappa^2\text{-trpd-2})(\text{dppm})]$ (**3a,b**). Sodium amalgam reduction of $[\text{MoI}_3(\text{trpd-2})]$ under N_2 in the presence of dppm results in a mixture of two *trans*-bis(dinitrogen) complexes (Scheme 6) with only four coordinated P groups, one P donor of the tripod phosphine arms being free. In the isomer denoted as $[\text{Mo}(\text{N}_2)_2(\kappa^2\text{-trpd-2})(\text{dppm})]$ (**3a**) two different P donor groups (P^iPr_2 and PPh_2) of the tripod are coordinated in the equatorial plane whereas in the other one two P^iPr_2 groups are coordinated at these positions (**3b**). By integration of the ^{31}P NMR spectrum isomer **3a** with coordinated PPh_2 and P^iPr_2 groups can be identified as the main product (ratio **3a**: **3b** ~ 6: 1; Supporting Information, Figure S5). A possible reason for this finding is the fact that coordination of one aromatic phosphine group enables π -backbonding which results in a lower energy as compared to coordination of two alkylphosphine groups.

$[\text{Mo}(\text{N}_2)_2(\kappa^2\text{-trpd-2})(\text{dmpm})]/[\text{Mo}(\text{N}_2)_2(\text{iso-}\kappa^2\text{-trpd-2})(\text{dmpm})]$ (**4a,b**). To reduce the steric demand of the diphosphine coligand and obtain a dinitrogen complex with a κ^3 -coordinated tripod the sodium amalgam reduction was repeated with the smaller coligand dmpm (Scheme 6). However, the reaction again led to a mixture of two coordination isomers, $[\text{Mo}(\text{N}_2)_2(\kappa^2\text{-trpd-2})(\text{dmpm})]$ (**4a**) and $[\text{Mo}(\text{N}_2)_2(\text{iso-}\kappa^2\text{-trpd-2})(\text{dmpm})]$ (**4b**), with one phosphine arm of the tripod ligand being free. Integration of the ^{31}P

NMR spectrum shows that both isomers **4a** and **4b** are formed in about equal quantities (Supporting Information, Figure S6).

$[\text{Mo}(\text{N}_2)_2(\kappa^2\text{-trpd-3})(\text{dppm})]$ (**5**) and $[\text{Mo}(\text{N}_2)_2(\kappa^2\text{-trpd-3})(\text{dmpm})]$ (**6**). Sodium amalgam reductions of $[\text{MoI}_3(\text{trpd-3})]$ under N_2 in the presence of dppm or dmpm both resulted in *trans*-bis(dinitrogen) complexes (**5** and **6**) with one tripod arm being free (Scheme 7).

Scheme 7



$[\text{Mo}(\text{N}_2)_2(\kappa^2\text{-tdppmm})(\text{dmpm})]$ (**7**). Sodium amalgam reduction of the complex $[\text{MoI}_3(\text{thf})\kappa^2\text{-(tdppmm)}]$ in the presence of the diphosphine ligand dmpm under N_2 was also found to lead to a *trans*-bis(dinitrogen) complex, *trans*- $[\text{Mo}(\text{N}_2)_2(\kappa^2\text{-tdppmm})(\text{dmpm})]$ (**7**), with one PPh_2 group of the tripod ligand being free (Scheme 7). Note that the analogous neopentyl tripod ligand tdppme along with coligands dmpm and dppm afforded the κ^3 -complexes $[\text{Mo}(\text{N}_2)(\text{tdppme})(\text{diphos})]$.²⁸ This difference is considered in more detail below.

2. Structural and Spectroscopic Characterization. A. X-ray Structure Determination. Information on the solid-state structures of compounds **1** and **2** was obtained from X-ray crystallography. Selected crystal structure data are collected in Table 1.

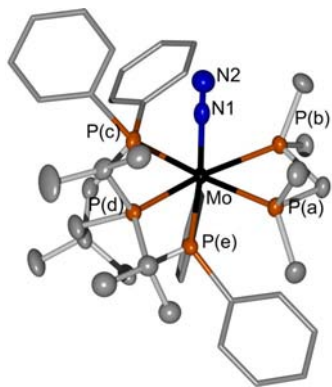
$[\text{Mo}(\text{N}_2)(\text{trpd-1})(\text{dmpm})]$ (**1**). Single crystals of complex **1** were grown by evaporation of a THF/pentane solution. The compound crystallizes in the space group $P2_1/n$. Figure 1 shows the structure of **1**. The octahedral complex has five coordinated phosphine groups. The two dimethylphosphine donors of dmpm as well as one PPh_2 and one P^iPr group of **trpd-1** are coordinated in the equatorial plane. The second PPh_2 group is bound in *trans* position to the N_2 ligand. The Mo– N_α distance (2.047(2) Å) and the N_α – N_β distance (1.055(3) Å) are both slightly shorter than in $[\text{Mo}(\text{N}_2)(\text{tdppme})(\text{dmpm})]$ (2.066(6) Å and 1.069(8) Å, respectively; cf. Table 2);²⁸ as in the latter complex the N–N distance of **1** is also shorter than in molecular dinitrogen (1.098 Å).⁴⁰

In comparing to the symmetric tdppme complex, we observe a deformation of the facial coordination of the **trpd-1** ligand. In complex $[\text{Mo}(\text{N}_2)(\text{tdppme})(\text{dmpm})]$ the two P–Mo–P angles from the equatorial tripod P atoms to the P atom in *trans* position to N_2 are almost equal (85.7° and 86.0°), and all

Table 1. Selected Crystal Data and Details on the Structure Determinations from Single Crystal Data of Compound 1 and Compound 2

	1	2
formula	C ₄₀ H ₃₇ MoN ₂ P ₅	C ₆₀ H ₆₅ MoP ₅
MW/g mol ⁻¹	816.67	1036.91
crystal system	monoclinic	monoclinic
space group	P2 ₁ /n	P2 ₁ /c
a/Å	12.3102(9)	12.3476(7)
b/Å	18.5529(9)	25.3230(19)
c/Å	20.8163(18)	18.3494(12)
β/deg	106.03 (1)	95.107(7)
V/Å ³	4569.3(6)	5714.7(7)
T/K	200(2)	200(2)
Z	4	4
D _{calc} /g cm ⁻³	1.187	1.205
μ/mm ⁻¹	0.489	0.405
min/max transmission	0.8215/0.9564	
θ _{max} /deg	25.95	27.00
measured reflections	36756	59603
unique reflections	8862	12112
R _{int}	0.0540	0.0612
reflections [F _o > 4σ(F _o)]	7566	10505
parameter	457	596
R ₁ ^a [F _o > 4σ(F _o)]	0.0332	0.0819
wR ₂ ^b [all data]	0.0837	0.1838
GOF	1.045	1.252
Δρ _{max} Δρ _{min} /e Å ⁻³	0.358, -0.702	1.388, -0.746

^aR₁ = ∑||F_o| - |F_c|| / ∑|F_o|. ^bwR₂ = [∑[w(F_o² - F_c²)²] / ∑[w(F_o²)²]]^{1/2}.

**Figure 1.** Single crystal structure of [Mo(N₂)(trpd-1)(dmpm)] (1); hydrogen atoms are omitted (displacement ellipsoids are drawn at the 50% probability level).

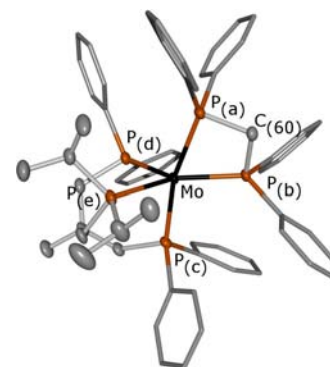
tripod bond lengths are in the range of Mo–P = 2.39–2.44 Å. The distortion in compound 1 is reflected by a difference of the angle between the diisopropyl phosphine donor P_d and the diphenylphosphine donor P_e in *trans* position to N₂ (87.3°) and the angle between the two arylphosphine donors P_c and P_e (83.6°). Moreover, the Mo–P_c bond (2.4130(6) Å) is shorter than the Mo–P_d bond (2.4428(5) Å). The angle between P_c and P_d in the equatorial plane is 85.2°, which is slightly larger than in the tdppme complex (82.3°). All of these observations indicate a larger steric demand of PⁱPr₂ as compared to PPh₂. The bite angle 67.4° of the coligand dmpm is almost similar to the angle in [Mo(N₂)(tdppme)(dmpm)] (66.9°).²⁸

[Mo(trpd-1)(dppm)] (2). Single crystals of compound 2 could be obtained by evaporation of a diethylether into a THF

Table 2. Selected Bond Distances and Angles of Compound 1

Bond Distances [Å]			
Mo–N(1)	2.047(2)	N(1)–N(2)	1.055(3)
Mo–P(a)	2.4653(6)	Mo–P(b)	2.4749(5)
Mo–P(c)	2.4130(6)	Mo–P(d)	2.4428(5)
Mo–P(e)	2.4439(5)		
Bond Angles [deg]			
N(1)–Mo–P(a)	87.87(5)	N(1)–Mo–P(b)	87.25(5)
N(1)–Mo–P(c)	91.43(5)	N(1)–Mo–P(d)	89.64(5)
N(1)–Mo–P(e)	174.35(5)		
P(e)–Mo–P(a)	97.319(18)	P(e)–Mo–P(b)	96.780(18)
P(e)–Mo–P(c)	83.593(2)	P(e)–Mo–P(d)	87.283(5)
P(b)–Mo–P(a)	67.444(2)	P(c)–Mo–P(b)	107.532(3)
P(d)–Mo–P(a)	99.836(3)	P(c)–Mo–P(d)	85.158(2)

solution of the complex. Figure 2 shows the structure of 2. The compound crystallizes in the space group P2₁/c. Selected bond lengths and angles are collected in Table 3.

**Figure 2.** Single crystal structure of [Mo(trpd-1)(dppm)] (2); hydrogen atoms are omitted (displacement ellipsoids are drawn at the 50% probability level). No indication of an agostic interaction between the Mo center and the C–H of one of the *i*Pr groups in P(e) could be found.**Table 3.** Selected Bond Distances and Angles of Compound 2

Bond Distances [Å]			
Mo–P(a)	2.4782(14)	Mo–P(b)	2.3986(13)
Mo–P(c)	2.3979(15)	Mo–P(d)	2.4511(16)
Mo–P(e)	2.5304(14)		
Bond Angles [deg]			
P(c)–Mo–C(60)	131.72	P(d)–Mo–C(60)	134.30
P(e)–Mo–C(60)	120.10		
P(e)–Mo–P(a)	105.81(5)	P(e)–Mo–P(b)	141.08(6)
P(c)–Mo–P(a)	166.48(5)	P(c)–Mo–P(b)	99.68(5)
P(d)–Mo–P(a)	104.24(5)	P(d)–Mo–P(b)	135.27(5)
P(e)–Mo–P(c)	84.51(5)	P(e)–Mo–P(d)	83.50(5)
P(c)–Mo–P(d)	85.32(5)	P(b)–Mo–P(a)	66.80(5)

The structure determination proves that compound 2 only contains five coordinated phosphine donor groups and no sixth ligand. The geometry shown in Figure 2 is best described as distorted trigonal bipyramidal with atoms P(b), P(d), and P(e) forming the trigonal plane and atoms P(a) and P(c) being in axial positions. Within the trigonal plane the angles [P(e)–Mo–P(b)] and [P(d)–Mo–P(b)] are 141° and 135° whereas the angle [P(e)–Mo–P(d)] is 83°, giving a sum of 359°. In

comparison to complex **1** the angles [P–Mo–P] within the tripod (83.5–85.3°) are more equal to each other, showing less distortion of the tripod coordination. The dppm bite angle (66.8°) is similar to the dmpm angle in complex **1**.

B. Vibrational Spectroscopy. Vibrational spectroscopy is ideally suited to monitor the activation of coordinated N_2 .^{10,12,14,41–44} The IR and Raman spectra of $[Mo(N_2)(trpd-1)(dmpm)]$ (**1**) (Figure 3) show the N–N stretch at $\nu = 1965$

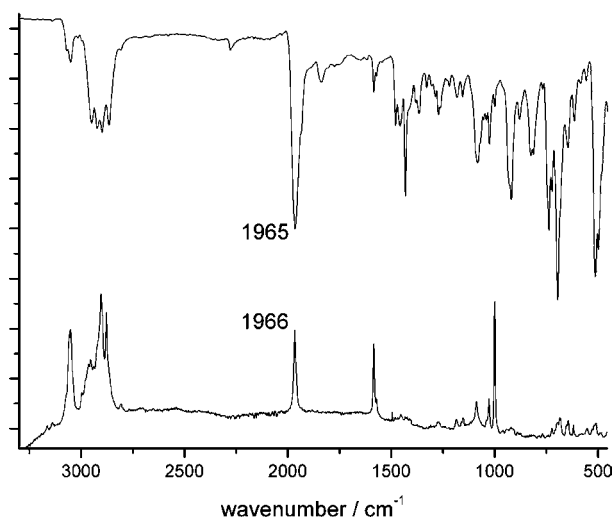


Figure 3. IR (top) and Raman (bottom) of $[Mo(N_2)(trpd-1)(dmpm)]$ (**1**).

cm^{-1} which indicates a moderately activated dinitrogen ligand. Because of the additional alkylphosphine donor, the electron density at the molybdenum center is higher as compared with $[Mo(N_2)(tdppme)(dmpm)]$, which exhibits a N–N stretch of $\nu = 1979\text{ cm}^{-1}$. The shift of the vibration at lower wavenumbers in compound **1** is in contrast to the shorter N–N bond length determined in the crystal structure of **1** (N–N = 1.055(3) Å) as compared with $[Mo(N_2)(tdppme)(dmpm)]$ (N–N = 1.069(8) Å) (vide supra).

Complex **2** does not show any vibrations of a bound N_2 ligand, in agreement with the structural and NMR data. The bis(dinitrogen) complexes **2** to **7** are coordinated by the respective tripod ligands in a κ^2 fashion and therefore exhibit symmetric and antisymmetric N–N stretches; the corresponding frequencies are collected in Table 4 (vibrational spectra are given in Supporting Information, Figures S7–S11). The intensity distribution observed in the infrared spectra (higher intensities for the antisymmetric stretches and lower intensities for the symmetric stretches; Raman spectra vice versa) qualitatively agree with the data obtained on *trans*-bis-(dinitrogen) complexes with two diphosphine ligands.^{14,44} In general it is observed that a larger number of alkyl phosphine groups results in a higher activation (lower frequency), although the frequency changes are smaller for the bis-(dinitrogen) complexes than for their mono(dinitrogen) counterparts. This is particularly evident for complexes **5** and **6** which only differ by the coligand, that is, in $[Mo(N_2)_2(\kappa^2-trpd-3)(dmpm)]$ (**6**) the asymmetric stretching frequency is only 10 cm^{-1} lower than in complex **5**, $[Mo(N_2)_2(\kappa^2-trpd-3)(dppm)]$.

C. ^{31}P NMR Spectroscopy. Information on the solution structures of the synthesized Mo(0) complexes was obtained from ^{31}P NMR spectroscopy. NMR spectroscopic data for all

Table 4. Infrared^a and Raman (Middle) N–N Stretching Wavenumbers^b

compound	$\nu(N-N)$ IR/ cm^{-1}	$\nu(N-N)$ RA/ cm^{-1}	number of alkyl phosphines
1 $[Mo(N_2)(trpd-1)(dmpm)]$	1965	1966	3
$[Mo(N_2)(tdppme)(dmpm)]$ ²⁸	1979	1980	2
$[Mo(N_2)(tdppme)(dppm)]$ ²⁸	2035	2040	0
4a, b $[Mo(N_2)_2(\kappa^2-trpd-2)(dmpm)]$	2009 s/1933 as		4/3
3a, b $[Mo(N_2)_2(\kappa^2-trpd-2)(dppm)]$	2019 s/1936 as		2/1
6 $[Mo(N_2)_2(\kappa^2-trpd-3)(dmpm)]$	2005 s/1925 as	2006	4
5 $[Mo(N_2)_2(\kappa^2-trpd-3)(dppm)]$	2006 s/1935 as	2005	2
7 $[Mo(N_2)_2(\kappa^2-tdppmm)(dmpm)]$	2018 s/1937 as	2018	2

^aSymmetric and antisymmetric stretching for bis(dinitrogen) complexes are given on the left. ^bThe number of alkyl phosphine groups coordinated to Mo is given on the right.

complexes is summarized in the Supporting Information, Table S1. The coupling constants derived from analysis of the spectra were checked by simulation of the ^{31}P NMR spectra.

$[Mo(N_2)(trpd-1)(dmpm)]$ (**1**). The ^{31}P NMR spectrum of **1** contains a set of five dddd-signals located at 47.3, 41.1, 40.3, –23.9, and –25.0 ppm, which are associated with the five P nuclei coupling among each other (cf. Figure 4). The signals could be assigned by comparison of the corresponding coupling constants. The resulting assignment was supported by the 1H - ^{31}P HMBC spectrum which allowed identifying the signal of the P^iPr_2 -group (Supporting Information, Figure S12). The signals at –23.9 ppm and –25.0 ppm are attributed to the two atoms P_a and P_b of the dmpm ligand which couple among each other with a constant of $^2J_{ab}^1 = 3.8\text{ Hz}$. The coupling consists of a metal- and a ligand-mediated contribution. The negative shift is in accordance with the high shielding of the P nuclei by the methyl groups, which was also observed for $[Mo(N_2)(tdppme)(dmpm)]$ exhibiting signals in the range between –22.5 to –23.5 ppm.²⁸ The signal at 40.3 ppm can be assigned to the aromatic P atom P_c in *trans* position to N_2 which couples via the metal to all other P atoms in *cis*-position with constants in the range between $^2J(cis) = -20.8$ to –27.3 Hz, resulting in a strongly overlapped dddd signal. The signal of the second aromatic P atom P_c is located at 41.1 ppm, and the signal of the diisopropyl P_d atom is found at 47.29 ppm. Both atoms couple with four other P atoms, corresponding to three coupling constants $^2J(cis)$ in the range between –20.8 to –27.3 Hz and two larger *trans* coupling constants $^2J(trans)$ of 93.5 and 86.8 Hz, respectively.

$[Mo(trpd-1)(dppm)]$ (**2**). The ^{31}P NMR spectrum of **2** contains three signals located at 48.9 ppm (dt), 40.6 ppm (t) and 33.8 ppm (br s) (Figure 5). The signal at 48.9 ppm can be assigned to the two aromatic P donors P_c and P_d of the tripod ligand. It is split through coupling with the signal at 40.6 ppm deriving from the P^iPr_2 group (P_e ; $J = -41.3\text{ Hz}$) and furthermore by weak coupling ($|J| = 6.7\text{ Hz}$) with the signal at 33.8 ppm being associated with the two P atoms P_a and P_b of dppm.

The signal of dppm appears as a broad singlet exhibiting three shoulders, from which again the coupling constant $|J| =$

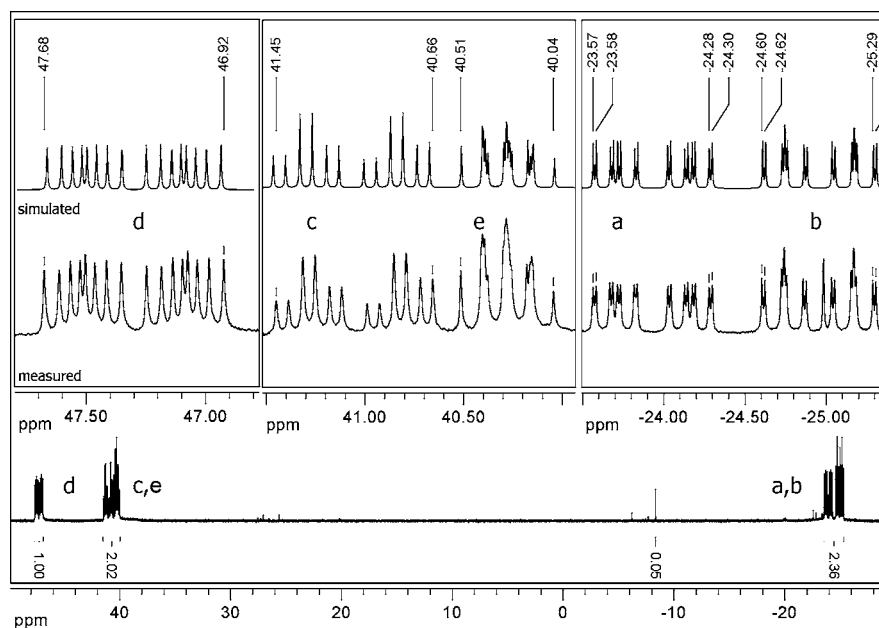


Figure 4. ^{31}P NMR spectrum of $[\text{Mo}(\text{N}_2)(\text{trpd-1})(\text{dmpm})]$ (1), detailed zoom and simulation with the derived coupling constants on top. Assignments of the atoms are given in Scheme 5.

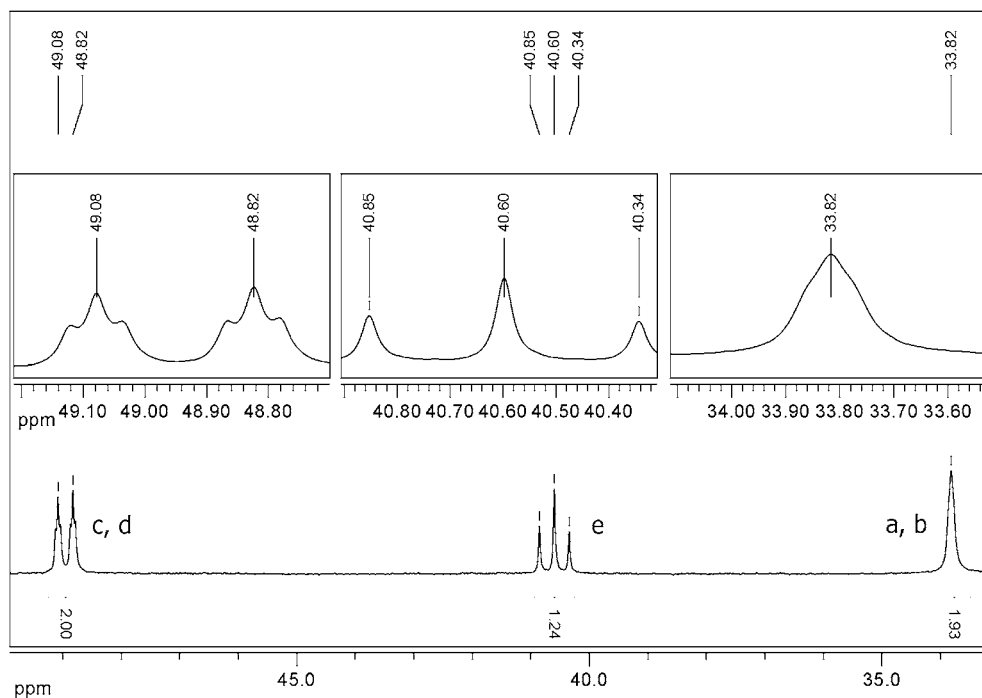


Figure 5. ^{31}P NMR spectrum of $[\text{Mo}(\text{trpd-1})(\text{dppm})]$ (2). Assignments of the atoms are given in Scheme 5.

6.7 Hz can be derived. Interestingly, the signals of P_e at 40.6 ppm and $P_{a,b}$ at 33.8 ppm exhibit no coupling among each other. Furthermore, no *trans* coupling constant in the usual range of $J = 100$ Hz is observed in the ^{31}P NMR spectrum of **2**. This unusual set of coupling constants, which is not observed in any other molybdenum(0) complex investigated in this work and in our earlier studies,^{26–28} can be attributed to the geometry shown in Figure 7. Assuming a rapid turnstile rotation of the dppm ligand,⁴⁵ the signals of the two P atoms P_a and P_b get averaged.

To validate this model, variable-temperature ^{31}P NMR spectra were recorded (Figure 6). All signals are temperature

dependent with respect to their positions and their linewidths. The strongest dependence is observed for the signal of $P_{a,b}$ at 33.8 ppm (300 K) which around 200 K becomes strongly broadened and disappears at lower temperatures. The signals $P_{c,d,e}$ of the tripod ligand, in contrast, are still visible. Because of the freezing point of the solvent thf-d_8 (164.8 K) we were not able to further cool down the sample until a new, static spectrum appears.

Referring to the structural model of Figure 7, it can be stated that the coupling between $P_{a,b}$ and P_e vanishes, and the coupling between $P_{a,b}$ and $P_{c,d}$ is weak ($|J| = 6.7$ Hz). For further discussion of this finding, a vector is defined from the

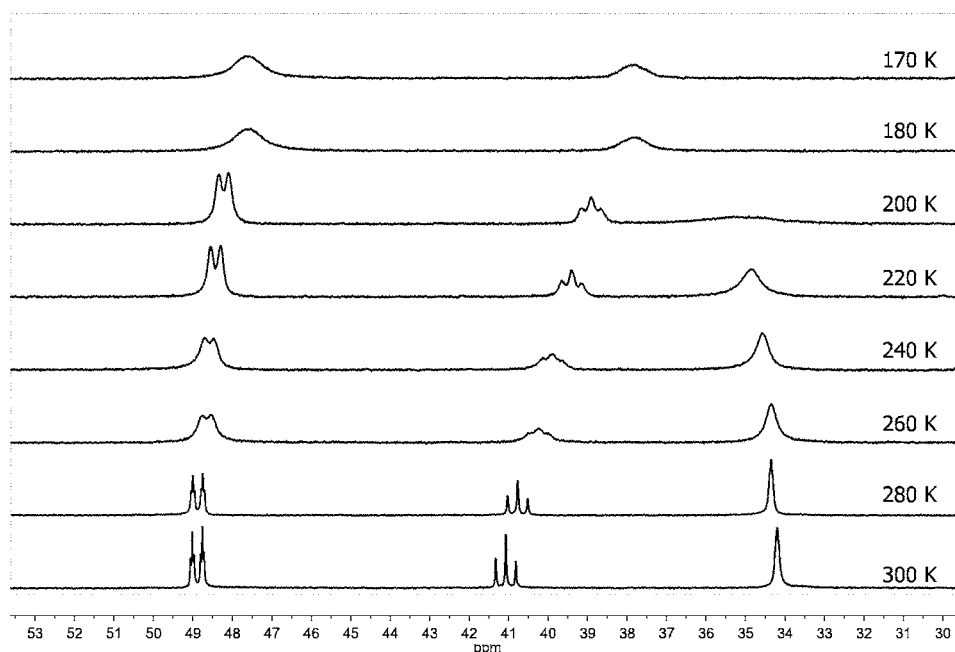


Figure 6. Variable-temperature ^{31}P NMR spectra of $[\text{Mo}(\text{trpd-1})(\text{dppm})]$ (**2**).

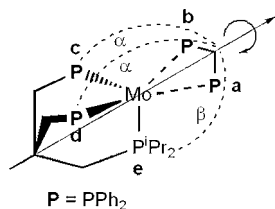


Figure 7. Turnstile rotation of the dppm ligand in $[\text{Mo}(\text{trpd-1})(\text{dppm})]$ (**2**) around an axis approximately perpendicular to the P_3 plane of **trpd-1**.

central C atom of the dppm ligand to the molybdenum atom representing the rotation axis of dppm. The angles α and β denote the positions of $\text{P}_{\text{c,d}}$ and P_{e} , respectively, with regard to this vector. Under the assumption that all $[\text{P}-\text{Mo}-\text{P}]$ tripod angles are 90° and the rotation axis goes through the center of the tripod ligand the angles α and β are 125.25° . However, because of the larger steric demand of the P^iPr_2 group as compared to the PPh_2 groups (vide supra), the angle β is supposed to be somewhat larger and the angle α somewhat smaller than 125° .

It is known that the sign of the $\text{P}-\text{Mo}-\text{P}$ coupling constants depends on the corresponding bond angle,²⁷ that is, the *trans* coupling constants (for $[\text{P}-\text{Mo}-\text{P}]$ angles around 180°) are large and positive, whereas the *cis* coupling constants (for $[\text{P}-\text{Mo}-\text{P}]$ angles around 90°) are smaller and negative. It thus follows that there has to be an angle between 180° and 90° at which the $\text{P}-\text{Mo}-\text{P}$ coupling constant vanishes. Obviously this situation is encountered in complex **2** for angle β , explaining the lack of coupling between atoms $\text{P}_{\text{a,b}}$ and P_{c} . The angles α , in contrast, have values that allow a weak, but nonvanishing coupling between $\text{P}_{\text{a,b}}$ and $\text{P}_{\text{c,d}}$.

Bis(dinitrogen) Complexes of the Tripod Ligands trpd-2, trpd-3, and tdppmm. For a bidentate coordination of the ligand **trpd-2** two different types of signal sets are expected. Correspondingly, the complexes **3a** and **4a** exhibit sets of four ddd signals while the more symmetric complexes **3b** and **4b** exhibit AA'XX' patterns.⁴⁶ The signals of the respective

uncoordinated third arms can be found in the negative range of the spectrum. The bis(dinitrogen) complexes **5** and **6** of ligand **trpd-3** and the bis(dinitrogen) complex **7** of ligand **tdppmm** exhibit AA'XX' patterns in the ^{31}P NMR spectrum as well. The assignments for one set of ddd signals deriving from **3a** and one AA'XX' set deriving from **3b** are given in detail as examples; all other data is summarized in Supporting Information, Table S1.

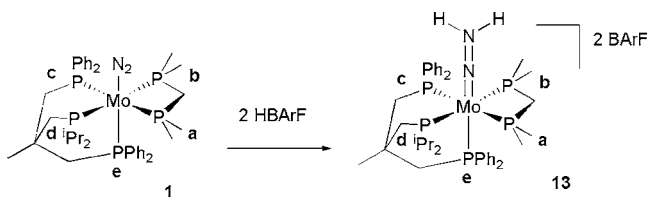
Complex $[\text{Mo}(\text{N}_2)_2(\kappa^2\text{-trpd-2})(\text{dppm})]$ (**3a**) exhibits a set of four ddd-signals. The two signals at 9.2 ppm and 10.9 ppm can be assigned to the dppm atoms $\text{P}_{\text{a,b}}$ while the signal at 40.2 ppm belongs to the diphenylphosphine donor P_{c} and the signal at 46.2 ppm to the diisopropyl phosphine donor P_{d} . Compound $[\text{Mo}(\text{N}_2)_2(\text{iso-}\kappa^2\text{-trpd-2})(\text{dppm})]$ (**3b**), in contrast, exhibits an AA'XX' spectrum with multiplets at 44.3 ppm and 9.4 ppm. Again the signals at 9.4 ppm can be assigned to the dppm atoms $\text{P}_{\text{a,b}}$ while the signal set at 44.3 ppm can be attributed to the $\text{P}_{\text{c,d}}$ P^iPr_2 groups of **trpd-2**. The signal of the respective uncoordinated third arm can again be found in the negative range at -3.6 ppm for **3a** (free P^iPr_2) and at -20.9 ppm for **3b** (free PPh_2). All spectra are displayed in the Supporting Information, Figures S5, S6, and S13–S15.

3. Reactivity with Acids. Of particular interest with respect to the application of the synthesized dinitrogen complexes in nitrogen fixation is their reactivity toward acids. Whereas the κ^2 tripod-coordinated $\text{Mo}(0)$ complexes **2–7** are bis(dinitrogen) complexes which react with acids under exchange of one dinitrogen ligand against the conjugate base of the acid employed for protonation,^{12,16} the monodinitrogen complex $[\text{Mo}(\text{N}_2)(\text{trpd-1})(\text{dmpm})]$ (**1**) has the potential of being protonated under retention of its ligand sphere, in analogy to the complex $[\text{Mo}(\text{N}_2)(\text{tdppme})(\text{dmpm})]$ investigated earlier.²⁸ Protonation of **1** with HOTf, H_2SO_4 , or HCl, however, did not lead to well-defined products. The only acid allowing generation and detection of the NNH_2 complex was HBARf (BARf = tetrakis[3,5-bis(trifluoromethyl)phenyl]borate).⁴⁷ The main advantage of this reagent is the low coordinating ability of the $[\text{BARf}]^-$ anion. The good solubility of $[\text{Mo}(\text{NNH}_2)(\text{trpd-}$

1)(dmpm)]BARF (13), however, also precluded isolation of this compound as a solid. The protonation reaction was therefore performed as an NMR experiment.

To this end, about 2.5 equiv of $[\text{H}(\text{OEt})_2]^+[\text{BARF}]^{-47}$ were added to a solution of **1** in CD_2Cl_2 , and the changes in the ^{31}P NMR spectrum were monitored. The presence of the five phosphine donor groups in the NNH_2 complex **13** is evident from retention of the AA'XX'M pattern (Supporting Information, Figure S16). Because of oxidation of the molybdenum center the signals of **13** are shifted to high field with respect to the N_2 complex **1**. Comparison of the ^{31}P NMR shifts between the latter complex and the NNH_2 complex **13** indicates a difference of $\Delta\delta = -5.0$ ppm and -7.2 ppm for the signals of P_a and P_b (Scheme 8) and $\Delta\delta = -17.5$ ppm and

Scheme 8



-12.0 ppm for the signals of P_c and P_d , respectively (cf Table 5). The largest chemical shift difference ($\Delta\delta = -46.7$ ppm) is

Table 5. ^{31}P -NMR Chemical Shifts of N_2 - and Corresponding NNH_2 Complexes with Pentaphosphine Ligand^a

δ / ppm	^{31}P NMR					^1H NMR NNH_2
	A	B	C	D	E	
[Mo(N_2)(trpd-1)(dmpm)] (1)	-23.93	-24.96	41.06	47.29	40.28	
[Mo(NNH_2)(trpd-1)(dmpm)] ²⁺ (13)	-28.93	-32.24	24.51	35.24	-6.53	9.4 / 10.8
Δ	-5	-7.28	-16.55	-12.05	-46.81	
[Mo(N_2)(tdppme)(dmpm)] ²⁺	-23	-23	39.5	39.5	40.2	
[Mo(NNH_2)(tdppme)(dmpm)] ²⁺ ²⁸	-27.4	-27.4	21.5	21.5	-4.38	9.2
Δ	-4.4	-4.4	-18	-18	-44.58	
[Mo(N_2)(dpepp)(dppm)] ²⁶	9.8	9.8	66.4	66.4	89.5	
[Mo(NNH_2)(dpepp)(dppm)] ²⁺ ²⁶	-2.9	-2.9	54.5	54.5	48.6	9.9
Δ	-12.7	-12.7	-11.9	-11.9	-40.9	

^aProton shifts are also given for the latter .

observed for P_e in *trans* position to N_2/NNH_2 . Very similar values were determined for the relative shifts of the two complexes [Mo(N_2)(tdppme)(dmpm)] and [Mo(NNH_2)(tdppme)(dmpm)]²⁺ ($\text{P}_{a,b}$ $\Delta\delta = -4.5$ ppm, $\text{P}_{c,d}$ $\Delta\delta = -18.0$ ppm, P_e $\Delta\delta = -44.4$ ppm).²⁸ The two protons of the NNH_2 group of **13** appear in the ^1H NMR spectrum at 9.4 and 10.8 ppm (cf Table 5). These positions are also very similar to those found for the complexes [Mo(NNH_2)(tdppme)(dmpm)]²⁺²⁸ and [Mo(NNH_2)(dpepp)(dppm)]²⁺²⁶ where the NNH_2 proton signals are located at 9.2 and 9.9 ppm, respectively. In contrast to these systems where the proton resonances appear as singlets, however, they are split in **13** because of the C_1 symmetry of this complex.

To obtain further information on the constitution of **13** a geometry optimization was performed (cf Figure 8). Cartesian coordinates of the resulting structure are collected and

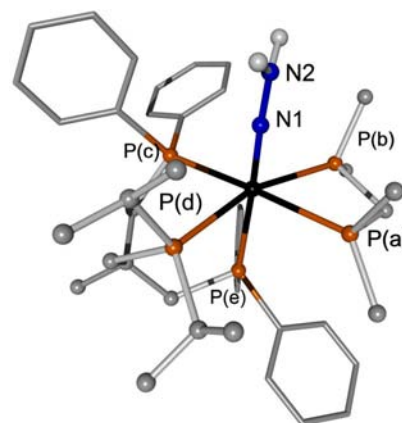


Figure 8. Optimized geometry of [Mo(NNH_2)(trpd-1)(dmpm)]²⁺ (**13**).

compared with those obtained for a model of the parent dinitrogen complex **1** as well as the related NNH_2 complex [Mo(NNH_2)(tdppme)(dmpm)]²⁺ in the Supporting Information, Tables S2–S4. The bond distances of the NNH_2 unit calculated for **13** are very similar to those obtained for [Mo(NNH_2)(dpepp)(dppm)]²⁺²⁶ and [Mo(NNH_2)(tdppme)(dmpm)]²⁺ (Supporting Information, Table S5).²⁸ Because of protonation, the N–N bond is lengthened to 1.32 Å in **13** with respect to **1** (N–N ext. 1.06 Å, calc. 1.16 Å, cf. Table 2 and Supporting Information, Table S5); simultaneously, the Mo–N bond is shortened to 1.77 Å (Mo–N of **1** ext. 2.05 Å, calc. 1.97 Å).

In agreement with the results from ^{31}P NMR spectroscopy (vide supra), the coordination environment of **1** is retained in **13**. According to the calculation the two protons of the NNH_2 group are oriented toward the P^iPr_2 and one of the PMe_2 groups, respectively (cf Figure.8). The ^1H NMR chemical shift difference observed experimentally for these protons indicates that the terminal NH_2 group of the NNH_2 ligand does not rotate. This supports the N=N double bond obtained for the NNH_2 ligand of **13**, similar to complex-bound diazene,⁴⁸ and agrees with our earlier formulation of Mo– NNH_2 systems as complexes of isodiazenes.^{14,15}

DISCUSSION, SUMMARY, AND CONCLUSION

In the preceding sections novel Mo(0) complexes supported by hybrid tripod ligands with mixed diarylphosphine/dialkylphosphine donor groups have been presented. Employing the hybrid tripod ligand **trpd-1** containing one diisopropyl phosphine group and two diphenyl phosphine groups, the molybdenum dinitrogen complex [Mo(N_2)(trpd-1)(dmpm)] (**1**) has been synthesized. With a NN stretch of $\nu = 1965$ cm^{-1} , the complex exhibits a moderate activation of the dinitrogen ligand. In comparison to the complex [Mo(N_2)(tdppme)(dmpm)] ($\nu = 1979$ cm^{-1}) presented earlier the activation is a little higher, which is due to the presence of one additional alkyl phosphine donor group. Note that the diisopropylphosphine group of the **trpd-1** ligand is coordinated in *cis*- and not in *trans*-position to the N_2 ligand. This is obviously due to the *trans*-effect, that is, the fact that diisopropylphosphine is a stronger σ -donor than diphenylphosphine. Importantly, dinitrogen complex **1** could be converted by protonation with $[\text{H}(\text{OEt})_2]^+\text{BARF}$ to the corresponding NNH_2 complex **13** for which retention of the five phosphine donor groups of **1** was demonstrated by ^{31}P NMR.

As found in our previous studies, diphosphines with a C_1 bridge are particularly well suited to stabilize dinitrogen complexes supported by tridentate or tripod ligands.^{26,28} For the tripod ligand **trpd-1**, replacement of dmpm with the bigger coligand dppm led to an N_2 free complex, which was identified as the five-coordinate complex $[Mo(trpd-1)(dppm)]$ (**2**). Apparently the steric demand of the P^iPr_2 in **trpd-1** in combination with the bigger dppm does not allow the coordination of a sixth ligand. It is remarkable that in the complex $[Mo(N_2)(tdppme)(dppm)]$,²⁸ which bears 10 phenyl rings, generation of the octahedral dinitrogen complex is still possible, whereas exchange of one diphenylphosphine for a bulkier diisopropylphosphine group prevents formation of the six-coordinate complex. The larger steric demand of P^iPr_2 as compared to PPh_2 is compatible with the Tolman cone angles of the respective monophosphines which are 160° for P^iPr_3 and 145° for PPh_3 .⁴⁹ To the best of our knowledge complex **2** is the first structurally characterized molybdenum(0) complex coordinated by five phosphine donor groups only.⁵⁰

The tripod ligands **trpd-2** (two P^iPr_2), **trpd-3** (three P^iPr_2), and **tdppmm** (three PPh_2) with an isobutyl backbone were found to be coordinated in a κ^2 -fashion, forming *trans*-bis(dinitrogen) complexes. The steric demand of the respective phosphine groups seems to be without any influence on these results because *all* isobutyl tripods **trpd-2**, **trpd-3**, and **tdppmm** were found to coordinate in a κ^2 mode. This finding rather appears to be due to the missing methyl group in comparison to the neopentyl based tripods which leads to a higher flexibility of the ligand whereby its capability to enforce a tridentate, facial coordination is lowered. This conclusion is supported by the fact that the all-diphenylphosphine tripod ligand **tdppmm** does not coordinate in a κ^3 fashion either, in contrast to its counterpart with a neopentyl-backbone, **tdppme**. Similar effects of an alkyl substitution within the backbone of the tripod ligand on its coordination mode (κ^2 vs κ^3) have been observed by Rosenberg and co-workers and attributed to steric influences of the side groups on the “kappticity” of the ligand.⁵¹ In contrast to the Mo(0) complexes, however, it appears that the κ^3 coordination of the isobutyl tripods **trpd-2** and **trpd-3** is well possible at the molybdenum(III) stage. This could be due to a higher electrophilicity of the Mo(III) as compared to the Mo(0) center, in particular leading to strong bonding of the highly nucleophilic diisopropylphosphine groups, and would be further supported by the fact that the isobutyl ligand **tdppmm**, with less electron-donating diphenylphosphine groups, is only coordinated in a κ^2 -fashion to Mo(III).

In summary, this study has provided important insights into the formation of molybdenum dinitrogen complexes supported by tripod ligands. In cases where κ^3 -complexes are formed protonation of the N_2 ligand is possible under retention of the pentaphosphine ligation, which represents the first step in the Chatt cycle and is a necessary condition for a dinitrogen complex to serve as a catalyst in the reduction and protonation of N_2 to ammonia. As shown in this paper, however, most tripod ligands only coordinate in a κ^2 fashion to the parent Mo(0) dinitrogen complex, which can be traced back to a combination of three factors, (i) steric demand of the phosphine substituents, (ii) electronic properties of the phosphine donors and, most importantly, (iii) flexibility of the ligand backbone. The fact that employing tripod ligands with an isobutyl backbone did not lead to a single Mo(0) complex exhibiting a κ^3 coordination in this study impressively demonstrates that the central methyl groups of the **tdppme** and

the **trpd-1** ligands are of paramount importance to guarantee a facial coordination, although the presence of this group renders the synthesis of tripod ligands with bulky substituents much more demanding.

EXPERIMENTAL SECTION

General Information. All reactions were carried out under N_2 -atmosphere using standard Schlenk-techniques or preparation in a MBRAUN glovebox. All solvents were dried and freshly distilled under Argon. All other reagents were used as commercially available without further purification. Silica gel (0.04–0.063 mm) from Merck was used for column chromatography. The compounds 1,1,1-tris-(chloromethyl)methane^{29,52,53} (**11**), diisopropyl phosphine,^{54,55} borane protected diisopropyl phosphine,⁵⁶ $[MoBr_3(thf)_3]$,³² $[MoCl_3(thf)_3]$,⁵⁷ $[MoI_3(thf)_3]$,³⁸ $[H(OEt)_2]BARf$ ^{47,58,59} were prepared according to the literature known procedures. 1,1,1-Tris-(diphenylphosphinomethyl)methane²⁹ (**tdppmm**) was prepared according to the literature procedure slightly varied by using *n*-butyllithium for deprotonation. For all deprotonation reactions a solution of 2.5 mol/L *n*-butyllithium in hexanes was used. The synthesis of **trpd-3** was performed with a 1.6 mol/L solution of *n*-butyllithium in hexanes. Elemental analyses were performed by using a Euro Vector CHNSO-element analyzer (Euro EA 3000). Samples were burned in sealed tin containers in a stream of oxygen. NMR spectra were recorded with a Bruker AVANCE 400 Pulse Fourier Transform spectrometer operating at frequencies of 400.13 MHz (1H), 161.98 MHz (^{31}P) 100.62 MHz (^{13}C). Referencing was performed either on the solvent residue signal ($CH_2Cl_2 = 5.32$ ppm, $C_6D_6 = 7.16$ ppm) or TMS ($\delta_{IH} = 0$ ppm) and 85% H_3PO_4 ($\delta_{31P} = 0$ ppm) serving as substitutive standards. Spectral simulations were performed by using the MestReC program package (Mestrelab Research, Santiago de Compostela, Spain). Vibrational spectroscopy: The FT-Raman spectra were recorded with a Bruker IFS 666/CS NIR FT-Raman spectrometer. Resonance-Raman-spectra were obtained by a XY-multichannel-Raman-Spectrometer with triple monochromator and CCD-detector by DILOR, Lille, France. A Ar^+/Kr^+ -laser by Spectra Physics, Darmstadt, with excitation wavelength from 454.5 to 647.1 nm was used as a light source. The resolution was between 2.5 and 0.8 cm^{-1} , depending on the excitation wavelength. Infrared spectra were recorded on a Bruker ALPHA FT-IR Spectrum with Platinum ATR setup. The DTA-TG measurements were performed in a nitrogen atmosphere (purity: 5.0) in Al_2O_3 crucibles using a STA-409CD thermobalance from Netzsch. All measurements were performed with a flow rate of 75 mL min^{-1} and were corrected for buoyancy and current effects. The instrument was calibrated using standard reference materials. Density functional theory (DFT) calculations were performed by using Gaussian 09. B3LYP was used as approximation functional. LANL2DZ for molybdenum and 6-311G for other atoms were used as basis sets.⁶⁰

Single Crystal Structure Analysis. Data collections for both compounds were performed with an imaging plate diffraction system (IPDS-1) from STOE & CIE using Mo- K_α -radiation ($\lambda = 0.71073\text{ \AA}$). The structure solutions were done with direct methods using SHELXS-97 and structure refinements were performed against $|F|^2$ using SHELXL-97.⁶¹ For compound **1** a numerical absorption correction was applied using X-Red Version 1.31 and X-Shape Version 2.11 of the Program Package X-Area.⁶² All non-hydrogen atoms except the disordered C atoms of lower occupancy in **1** were refined with anisotropic displacement parameters. All hydrogen atoms were positioned with idealized geometry (in compound **1** methyl H atoms allowed to rotate but not to tip) and were refined with fixed isotropic displacement parameters [$U_{eq}(H) = -1.2 \cdot U_{eq}(C)$] (1.5 for methyl H atoms) using a riding model. In compound **1** one of the diisopropyl groups is disordered over two sites and was refined using a split model (sof: 0.80:0.20). The structure of both compounds contains some additional amount of THF, which is disordered and for which no reasonable structure model was found.⁶³ Therefore, the data were corrected for disordered solvent using the SQUEEZE option in Platon. The electron count is in accordance with about half a THF

molecule per complex in **1** and about one-quarter of THF in **2**. All crystals investigated for **2** were always slightly nonmerohedral twinned but both individuals cannot be separated successfully and therefore, the twinning was not considered in the structure determination. However, this is the reason for the relatively high reliability factors and the highest residual peak in the electron density map which does not originate from absorption effects. Details of the structure determination are given in Table 1.

CCDC-940376 (**1**) and CCDC-940377 (**2**) contain the supplementary crystallographic data for this paper. These data can be obtained free of charge from the Cambridge Crystallographic Data Centre via <http://www.ccdc.cam.ac.uk/>.

Me-C(CH₂Cl)₂(CH₂PⁱPr₂-BH₃)₂ (9**).** A 3.24 g portion (24.5 mmol) of H-PⁱPr₂-BH₃ has been deprotonated by 9.8 mL of *n*-butyllithium (1 equiv) in 20 mL of THF at 0 °C. The mixture was stirred for 2 h, warmed to room temperature and added to 4.47 g (24.5 mmol) of Me-C(CH₂Cl)₃ (**8**) in 20 mL of THF. The mixture was stirred at ambient temperature for 12 h, afterward the reaction was quenched with 10 mL of H₂O. The water was removed syringe and extracted twice with 10 mL of diethyl ether. Evaporation of the solvent in vacuo gave a colorless liquid which was purified by column chromatography (toluene:cyclohexane/1:0.7/Rf = 0.54). Yield: 4.28 g (15.8 mmol, 64%) Anal. Calc. for C₁₁H₂₆BCl₂P₂: C, 48.8; H, 9.7; found: C, 49.0; H, 10.0. IR (ATR): 2970–2870, 2380–2347 (BH), 1460 (P–C), 1432 (P–C) cm⁻¹. ¹H NMR (400.13 MHz, CD₂Cl₂, 300 K, {³¹P, ¹¹B CPD}): δ = 3.71 (dd, 4H, CH₂-Cl, J = 11.1 Hz), 1.98 (sep, 2H, CH-(CH₃)₂, ³J = 7.1 Hz), 1.80 (s, 2H, CH₂-PⁱPr₂), 1.27 (s, 3H, C_q-CH₃), 1.18 (dd, 12H, CH-CH₃, J = 3.8, 7.1 Hz), 0.49 (s, 3H, -BH₃) ppm. ³¹P NMR (161.98 MHz, CD₂Cl₂, 300 K, H₃PO₄) δ = 27.9 (br q, 1P, PⁱPr₂-BH₃, J = 50.5 Hz, 108.3 Hz) ppm. ¹³C NMR (100.62 MHz, CD₂Cl₂, 300 K): δ = 51.5 (d, 2C, CH₂-Cl, J = 6.3 Hz), 40.4 (s, 1C, C-quart.), 24.0 (d, 2C, CH-CH₃, J = 24.9 Hz), 23.8 (d, 1C, CH₂-P, J = 34.1 Hz), 21.6 (d, 1C, C_q-CH₃), 16.7 (d, 4C, CH-CH₃) ppm.

Me-C(CH₂PPh₂)₂(CH₂PⁱPr₂-BH₃)₂ (10**).** A 4.25 g portion of (22.9 mmol) H-PPh₂ was deprotonated with 9.20 mL of *n*-butyllithium (1 equiv) in 20 mL of THF and added to 2.45 g of (9.04 mmol) Me-C(CH₂Cl)₂(CH₂PⁱPr₂-BH₃) (**9**) in 40 mL of THF by dropping funnel. The reaction mixture was stirred for 18 h, hydrolyzed by addition of 20 mL of H₂O, afterward the water was removed by syringe and extracted twice with diethyl ether. The solvent was removed in vacuo, and the crude product was purified by column chromatography (cyclohexane: ethylacetate/12:1/Rf = 0.71). Yield: 2.08 g (3.65 mmol, 40%) Anal. Calc. for C₃₅H₄₆BP₃: C, 73.7; H, 8.1; found: C, 73.9; H, 8.4. IR (ATR): 3070, 3050, 2954–2880, 2370–2340 (BH), 1480 (P–C), 1432 (P–C) cm⁻¹. ¹H NMR (400.13 MHz, CD₂Cl₂, 300 K): δ = 7.29 (m, 20H, CH phenyl), 2.51 (ddd, 4H, diastereotope H CH₂PPh₂, J = 14.2 Hz, ⁴J_{HP} = 2.8 Hz), 1.74 (sep, 2H, CH-(CH₃)₂), 1.70 (d, 2H, CH₂-PⁱPr₂, J = 11.4 Hz), 1.10 (s, 3H, C_q-CH₃), 1.19 (m, 12H, CH-CH₃), 0.49 (br m, 3H, -BH₃) ppm. ³¹P NMR (161.98 MHz, CD₂Cl₂, 300 K, H₃PO₄) δ = 26.9 (br d, 1P, PⁱPr₂), -24.5 (s, 2P, PPh₂) ppm. ¹³C NMR (100.62 MHz, CD₂Cl₂, 300 K): δ = 139.8 (m, 4C, C_q arom.), 133.9 (d, 8C, CH_o arom., ²J_{CP} = 20.2 Hz), 128.6–128.3 (m, 12C, CH_{mp} arom.), 42.9–42.6 (m, 2C, CH₂-PPh₂), 38.7 (m, 1C, C_q-CH₃), 32.2–31.8 (m, 1C, CH₂-PⁱPr₂), 28.2 (m, 1C, C_q-CH₃), 24.1 (d, 2C, CH-CH₃, ¹J_{CP} = 34.0 Hz), 16.8 (d, 4C, CH-CH₃, ²J_{CP} = 30.5 Hz) ppm.

Me-C(CH₂PPh₂)₂(CH₂PⁱPr₂)₂ (trpd-1). A 1.60 g portion of (2.8 mmol) Me-C(CH₂PPh₂)₂(CH₂PⁱPr₂-BH₃) (**10**) was stirred in 15 mL of degassed morpholine at 100 °C for 6 h, afterward the morpholine was removed in vacuo at 50 °C. The crude product was refluxed with 10 mL of methanol leading to a white precipitate which was filtered off and dried in vacuo. Yield: 1.25 g (2.25 mmol, 80%) Anal. Calc. for C₃₅H₄₃P₃: C, 75.5; H, 7.8; found: C, 75.8; H, 7.8. IR (ATR): 3070, 3045, 2960–2860, 1480 (P–C), 1432 (P–C) cm⁻¹. ¹H NMR (400.13 MHz, CD₂Cl₂, 300 K): δ = 7.44–7.27 (m, 20H, CH phenyl), 2.53 (ddd, 4H, diastereotope CH₂-PPh₂, J = 14.2 Hz, ⁴J_{HP} = 3.1 Hz), 1.67 (d sep, 2H, CH-CH₃, J = 7.1 Hz, ²J_{HP} = 3.1 Hz), 1.70 (d, 2H, CH₂-PⁱPr₂, ²J_{HP} = 5.5 Hz), 1.08 (s, 3H, CH₂-CH₃), 0.99 (dd, 12H, CH-CH₃, J = 3.8, 7.1 Hz, ³J_{HP} = 14.0 Hz) ppm. ³¹P NMR (161.98 MHz, CD₂Cl₂, 300 K): δ = -7.6 (s, 1P, PⁱPr₂) -25.1 (s, 2P, PPh₂) ppm. ¹³C

NMR (100.62 MHz, CD₂Cl₂, 300 K): δ = 140.3 (m, 4C, C_q arom.), 133.9, 133.0 (2d, 8C, CH_o arom., ²J_{CP} = 20.2 Hz), 128.4–128.3 (m, 12C, CH_{mp} arom.), 42.9–42.6 (m, 2C, CH₂-PPh₂), 37.9–37.7 (m, 1C, C_q-CH₃), 37.0–36.7 (m, 1C, CH₂-PⁱPr₂), 28.2 (q, 1C, C_q-CH₃, ³J_{CP} = 9.6 Hz), 23.9 (d, 2C, CH-CH₃, ¹J_{CP} = 12.4 Hz), 19.9 (d, 2C, CH-CH₃, ²J_{CP} = 14.5 Hz), 19.1 (d, 2C, CH-CH₃, ²J_{CP} = 10.6 Hz) ppm.

H-C(CH₂Cl)(CH₂PⁱPr₂-BH₃)₂ (12**).** A 4.91 g portion of (37.2 mmol) H-PⁱPr₂-BH₃ has been deprotonated by 14.9 mL of *n*-butyllithium (1 equiv) in 20 mL of THF at 0 °C. The mixture was stirred for 2 h, warmed to room temperature and added to 3.0 g of (18.6 mmol) H-C(CH₂-Cl)₃ (**11**) in 10 mL of THF by dropping funnel. The mixture was stirred for 16 h at room temperature and hydrolyzed with 10 mL of H₂O, afterward the water was removed by syringe and extracted twice with diethyl ether. The solvent was removed in vacuo, and the crude product was purified by column chromatography (toluene:cyclohexane/1:1/Rf = 0.34). Yield: 4.80 g (13.6 mmol, 73%) Anal. Calc. for C₁₆H₄₁B₂ClP₂: C, 54.5; H, 11.7; found: C, 55.0; H, 12.3. IR (ATR): 2960–2860, 2370–2348 (BH), 1458 (P–C), 1432 (P–C) cm⁻¹. ¹H NMR (400.13 MHz, CD₂Cl₂, 300 K): δ = 3.90 (d, 2H, CH₂-Cl, ³J = 4.1 Hz), 2.54 (m, 1H, CH-(CH₃)₃), 2.07–1.76 (m, 8H, 2 × CH₂-PⁱPr₂, 4 × CH-CH₃), 1.20–1.14 (m q, 24H, CH-CH₃), 0.36 (br q, 6H, -BH₃) ppm. ³¹P NMR (161.98 MHz, CD₂Cl₂, 300 K, H₃PO₄) δ = 30.9 (br q, 2P, PⁱPr₂) ppm. ¹³C NMR (100.62 MHz, CD₂Cl₂, 300 K): δ = 50.8 (tr, 1C, CH₂-Cl), 33.3 (tr, 1C, CH-(CH₃)₃), 23.1, 23.2 (2d, 2C, CH₂-PⁱPr₂, ¹J_{CP} = 28.2 Hz), 23.1, 23.2 (2d, 4C, CH-CH₃, ¹J_{CP} = 33.8 Hz), 16.8–16.4 (m, 8C, CH-CH₃) ppm.

H-C(CH₂PⁱPr₂)₂(CH₂PPh₂) (trpd-2). A 1.45 g portion of (7.80 mmol) H-PPh₂ was deprotonated with 3.12 mL of *n*-butyllithium (1 equiv) in 20 mL of THF and added to 2.50 g of (7.09 mmol) H-C(CH₂Cl)(CH₂PⁱPr₂-BH₃)₂ (**11**) in 40 mL of THF by dropping funnel. The reaction mixture was stirred for 16 h, hydrolyzed by addition of 20 mL of H₂O, afterward the water was removed by syringe and extracted twice with dichloromethane. The solvent was removed in vacuo and the crude product was purified by column chromatography (cyclohexane:ethylacetate/3:1/Rf = 0.68). Afterward the viscous product was stirred in morpholine for 9 h at 100 °C. The morpholine was removed, and the product was dried in vacuo for 24 h. Yield: 1.7 g (3.60 mmol, 46%) Anal. Calc. for C₂₈H₄₅P₃: C, 70.9; H, 9.6; found: C, 70.6; H, 9.8. IR (ATR): 3063, 3045, 2960–2860, 1480 (P–C), 1458 (P–C), 1431 (P–C) cm⁻¹. ¹H NMR (400.13 MHz, CD₂Cl₂, 300 K): δ = 7.51–7.28 (m, 10H, CH phenyl), 2.40 (d, 2H, CH₂-PPh₂, ³J = 6.7 Hz), 1.77–1.60 (m, 8H, 2 × CH₂-PⁱPr₂, 4 × CH-CH₃), 1.58–1.48 (m, 1H, CH-(CH₂)₃), 1.04–0.95 (m, 24H, CH-CH₃) ppm. ³¹P NMR (161.98 MHz, CD₂Cl₂, 300 K, H₃PO₄) δ = -3.6 (s, 2P, PⁱPr₂), -20.8 (s, 1P, PPh₂) ppm.

H-C(CH₂PⁱPr₂)₃ (trpd-3). A 2.66 g portion of (22.55 mmol) H-PⁱPr₂-BH₃ has been deprotonated by 14.1 mL of *n*-butyllithium (1 eq, 1.6 mol/L) in 20 mL of THF at 0 °C. The mixture was stirred for 2 h, warmed to room temperature and added to 1.17 g of (7.72 mmol) H-C(CH₂-Cl)₃ (**11**) in 20 mL of THF by dropping funnel. The mixture was stirred for 14 h at room temperature and hydrolyzed with 20 mL of H₂O, afterward the water was removed by syringe and extracted twice with diethyl ether. The solvent was removed, and the slightly green liquid was dried in vacuo. Yield: 2.60 g (6.40 mmol, 88%) Anal. Calc. for C₂₂H₄₉P₃: C, 65.0; H, 12.2; found: C, 64.7; H, 12.1. IR (ATR): 2947, 2920, 2865, 1460 (P–C) cm⁻¹. ¹H NMR (400.13 MHz, CD₂Cl₂, 300 K): δ = 1.75–1.53 (m, 6H, 6 × CH-CH₃), 1.48–1.38 (br m, 1H CH-(CH₂)₃), 1.45 (br d, 6H, CH₂-PⁱPr₂), 1.06–1.00 (m, 36H, CH-CH₃) ppm. ³¹P NMR (161.98 MHz, CD₂Cl₂, 300 K, H₃PO₄) δ = -3.27 (s, 3P, PⁱPr₂) ppm.

[Mo₃(trpd-X)]. A equimolar suspension of tripod ligand and [Mo₃(thf)₃] (typical amount of [Mo₃(thf)₃]: 0.5–1 g) in 20 mL of THF was stirred for 18 h at room temperature. The dark red solution was reduced in vacuo to a quantity of 5 mL and a dark red precipitate was formed by adding 40 mL of diethylether. In case of trpd-3 precipitation was effected by addition of 40 mL of hexanes. The precipitate was filtered and dried in vacuo.

[Mo₃(trpd-1)]: 620 mg of (900 μmol) [Mo₃(thf)₃] was reacted with 500 mg of (900 μmol) trpd-1. Yield: 700 mg (0.677 mmol, 75%)

Anal. Calc. for $C_{35}H_{43}I_3MoP_3$: C, 40.7; H, 4.2; I, 36.8; found: C, 40.2; H, 4.2; I, 36.3. IR (ATR): 3050, 2970, 2860, 1480 (P–C), 1460 (P–C), 1432 (P–C) cm^{-1} .

[$MoI_3(trpd-2)$]: 990 mg of (1.43 mmol) [$MoI_3(thf)_3$] was reacted with 680 mg of (1.43 mmol) **trpd-2**. Yield: 950 mg (0.340 mmol, 69%) Anal. Calc. for $C_{28}H_{45}I_3MoP_3$: C, 35.4; H, 4.8; I, 40.0; found: C, 35.1; H, 5.1; I, 40.4. IR (ATR): 3050, 2960, 2869, 1620, 1480 (P–C), 1460 (P–C), 1432 (P–C) cm^{-1} .

[$MoI_3(trpd-3)$]: 1.36 g of (1.97 mmol) [$MoI_3(thf)_3$] was reacted with 800 mg of (1.97 mmol) **trpd-3**. Yield: 670 mg (0.758 mmol, 39%) Anal. Calc. for $C_{22}H_{49}I_3MoP_3$: C, 29.9; H, 5.6; I, 43.1; found: C, 29.7; H, 5.7; I, 43.1. IR (ATR): 2970–2869, 1455 (P–C) cm^{-1} .

[$MoI_3(thf)(tdppmm)$]: 680 mg of (980 μ mol) [$MoI_3(thf)_3$] was reacted with 600 mg of (980 μ mol) **tdppmm**. Yield: 740 mg (0.640 mmol, 65%) Anal. Calc. for $C_{44}H_{45}I_3MoOP_3$: C, 45.6; H, 3.9; I, 32.8; found: C, 45.3; H, 3.9; I, 33.2. IR (ATR): 3050, 2960–2855, 1480 (P–C), 1434 (P–C) cm^{-1} .

Reduction under N_2 . All reductions to dinitrogen complexes were performed in similar fashion. A suspension of the respective [$MoI_3(trpd)$] complex (typical 500 mg) and an equimolar amount of dppm or dmpm as coligand in 30 mL of THF were added to sodium amalgam (300 mg Na, 3 mL Hg) and stirred under nitrogen for 24 h at room temperature. The solution was decanted from amalgam, filtrated and reduced to 5 mL. After addition of 5 mL of methanol and further reduction of the volume to 5 mL (repeated twice) a red precipitate or viscous product could be obtained.

[$Mo(N_2)(trpd-1)(dmpm)$] (**1**). A 500 mg portion of (480 μ mol) [$MoI_3(trpd-1)$] was reacted with 65.8 mg of (0.48 mmol) dmpm as described above. Yield: 105 mg (0.129 mmol, 26%). Anal. Calc. for $C_{40}H_{57}MoN_2P_5$: C, 58.8; H, 7.0; N, 3.4 found: C, 58.2; H, 7.0; N, 3.0. IR (ATR): 3056, 2952–2862, 1965 (NN), 1480 (P–C), 1433 (P–C) cm^{-1} . 1H NMR (400.13 MHz, C_6D_6 , 300 K): δ = 7.86–6.78 (m, 20H, CH arom.), 3.76 (m, 1H, CH_2 dmpm), 3.41 (m, 1H, CH_2 dmpm), 2.78–2.73 (br t, 1H, $CH-CH_3$), 2.48–2.44 (br t, 1H, CH_2-PPh_2), 2.25–2.20 (br d, 1H, CH_2-PPh_2), 2.00 (d, 3H, CH_3 dmpm, J = 4.8 Hz), 1.89 (br t, 2H, CH_2-PPh_2), 1.80–1.77 (m, 2H, $CH_2-P^iPr_2$), 1.72 (d, 3H, CH_3 dmpm, J = 5.0 Hz), 1.45 (m, 1H, $CH-CH_3$), 1.41 (d, 3H, CH_3 dmpm, J = 4.8 Hz), 1.36–1.25 (m, 12H, $CH-CH_3$, C_qCH_3), 1.10–1.08 (m, 3H, $CHCH_3$), 0.61 (d, 3H, CH_3 dmpm, J = 5.0 Hz) ppm. ^{31}P NMR (161.98 MHz, C_6D_6 , 300 K) δ = 47.3 (dddd, 1P, P_{cb} , J = –12.6, –22.4, –30.5, 86.8 Hz), 41.1 (dddd, 1P, P_c , J = –12.6, –27.3, –27.3, 93.5 Hz), 40.3 (dddd, 1P, P_{cb} , J = –20.8, –22.4, –24.4, –27.3 Hz), –23.9 (dddd, 1P, P_{cb} , J = 3.8, –20.8, 30.6, 93.5 Hz), –24.9 (dddd, 1P, P_{cb} , J = 3.8, –24.4, –27.9, 86.8 Hz) ppm.

[$Mo(trpd-1)(dppm)$] (**2**). A 400 mg portion of (390 μ mol) [$MoI_3(trpd-1)$] was reacted with 148 mg of (390 μ mol) dppm as described above. Yield: 200 mg (0.129 mmol, 45%). Anal. Calc. for $C_{60}H_{65}MoP_5$: C, 69.5; H, 6.3; found: C, 69.0; H, 7.0. IR (ATR): 3050, 2950–2860, 1481 (P–C), 1430 (P–C) cm^{-1} . 1H NMR (400.13 MHz, C_6D_6 , 300 K): δ = 7.73–7.60 (m, 20H, CH arom.), 6.88 (m, 20H, CH arom.), 5.28 (br t, 2H, CH_2 dppm), 2.58–2.22 (dd, 4H, CH_2-PPh_2), 1.62 (d, 2H, $CH_2-P^iPr_2$), 1.58 (m, 2H, $CH-CH_3$), 1.26 (s, 3H, C_qCH_3), 1.26–1.19 (dd, 6H, $CH-CH_3$), 0.81–0.77 (dd, 6H, $CH-CH_3$) ppm. ^{31}P NMR (161.98 MHz, C_6D_6 , 300 K) δ = 48.9 (dt, 2P, P_{cb} , $|J|$ = 6.7, J = –41.3 Hz), 40.6 (t, 1P, P_c , J = –41.3 Hz), 33.8 (br s, 2P, $P_{a,b}$, $|J|$ = 6.7 Hz) ppm.

trans-[$Mo(N_2)_2(\kappa^2-trpd-2)(dppm)$] (3a, b**)**. A 500 mg portion of (0.49 mmol) [$MoI_3(trpd-2)$] was reacted with 189 mg of (0.49 mmol) dppm as described. A red precipitate could be obtained which was determined as a mixture of two coordination isomers by ^{31}P NMR spectroscopy. Yield: 100 mg (0.098 mmol, 20%)

IR (ATR): 3049, 2960, 2012 (NN), 1936 (NN), 1480 (P–C), 1430 (P–C) cm^{-1} . 1H NMR (400.13 MHz, C_6D_6 , 300 K): **3a** δ = 7.85–7.48 (m, 10H, CH arom), 7.34–6.90 (m, 20H, CH arom), 2.66 (br d, 2H, CH_2-PPh_2), 2.58–2.44 (br t, 2H, CH_2 dppm), 2.05 (m, 1H, $CH-(CH_2)_3$), 1.84–1.74 (m, 4H, $CH-CH_3$), 1.72–1.57 (m, 4H, $CH_2-P^iPr_2$), 1.23–1.15 (m, 24H, $CH-CH_3$) ppm. **3b** δ = 7.85–7.48 (m, 10H, CH arom), 7.34–6.90 (m, 20H, CH arom), 2.58–2.44 (br t, 2H, CH_2 dppm), 2.05 (m, 1H, $CH-(CH_2)_3$), 1.85 (br d, 2H, CH_2-PPh_2), 1.84–1.74 (m, 4H, $CH-CH_3$), 1.72–1.57 (m, 4H, $CH_2-P^iPr_2$), 1.23–

1.15 (m, 24H, $CH-CH_3$) ppm. ^{31}P NMR (161.98 MHz, C_6D_6 , 300 K) **3a** δ = 46.2 (ddd, 1P, P_{cb} , J = 15.1, –27.1, 102.8 Hz), 40.2 (ddd, 1P, P_c , J = 10.6, –24.7, 104.5 Hz), 10.9 (ddd, 1P, P_{cb} , J = 15.1, –24.7, 102.8 Hz), 9.2 (ddd, 1P, P_{cb} , J = 15.1, –27.1, 104.5 Hz), –3.6 (s, 1P, P_c) ppm. **3b** δ = 44.3 (m, 2P, P_{cb} , J = 12.9, 15.2, –25.9, 102.9 Hz), 9.4 (m, 2P, $P_{a,b}$, J = 12.9, 15.2, –25.9, 102.9 Hz), –20.9 (s, 1P, P_c) ppm.

trans-[$Mo(N_2)_2(\kappa^2-trpd-2)(dmpm)$] (4a, b**)**. A 600 mg portion of (0.63 mmol) [$MoI_3(trpd-2)$] was reacted with 85.8 mg of (0.63 mmol) dmpm as described. A dark red oily precipitate could be obtained which was extracted by 20 mL of benzene which was evaporated in vacuo. A mixture of two coordination isomers could be determined by ^{31}P NMR spectroscopy. Yield: 80 mg (0.11 mmol, 17%)

IR (ATR): 3053, 2960–2865, 2009 (NN), 1933 (NN), 1460 (P–C), 1430 (P–C) cm^{-1} . 1H NMR (400.13 MHz, C_6D_6 , 300 K): **4a** δ = 7.70–7.08 (m, 10H, CH arom), 3.67–3.53 (m, 2H, CH_2 dmpm), 2.89 (br d, 2H, CH_2-PPh_2), 2.16 (m, 1H, $CH-(CH_2)_3$), 1.73–1.65 (m, 4H, $CH-CH_3$), 1.48–1.33 (br d, 4H, $CH_2-P^iPr_2$), 1.31–1.03 (m, 36H, 8 \times $CH-CH_3$, 4 \times CH_3 dmpm) ppm. **4a** δ = 7.70–7.08 (m, 10H, CH arom), 3.67–3.53 (m, 2H, CH_2 dmpm), 2.16 (m, 1H, $CH-(CH_2)_3$), 1.85 (br d, 2H, CH_2-PPh_2), 1.73–1.65 (m, 4H, $CH-CH_3$), 1.48–1.33 (br d, 4H, $CH_2-P^iPr_2$), 1.31–1.03 (m, 36H, 8 \times $CH-CH_3$, 4 \times CH_3 dmpm) ppm. ^{31}P NMR (161.98 MHz, C_6D_6 , 300 K) **4a** δ = 51.5 (ddd, 1P, P_{cb} , J = 11.5, –26.4, 110.2 Hz), 42.7 (ddd, 1P, P_c , J = 11.5, –28.3, 106.0 Hz), –17.9 (ddd, 1P, P_{cb} , J = 4.1, –28.3, 107.7 Hz), –20.8 (ddd, 1P, P_{cb} , J = 4.2, –26.4, 106.0 Hz), –5.6 (s, 1P, P_c) ppm. **4b** δ = 50.2 (m, 2P, P_{cb} , J = 7.6, 10.8, –27.1, 107.7 Hz), –21.7 (m, 2P, $P_{a,b}$, J = 7.6, 10.8, –27.1, 107.7 Hz), –22.8 (s, 1P, P_c) ppm.

trans-[$Mo(N_2)_2(\kappa^2-trpd-3)(dppm)$] (5**)**. A 370 mg portion of (0.42 mmol) [$MoI_3(trpd-3)$] was reacted with 161.4 mg of (0.42 mmol) dppm as described above. Yield: 80 mg (0.085 mmol, 20%)

Anal. Calc. for $C_{47}H_{71}MoN_4P_5$: C, 59.9; H, 7.6; N, 5.9 found: C, 59.8; H, 7.2; N, 5.8.

IR (ATR): 3052, 2960–2866, 2006 (NN), 1935 (NN), 1477 (P–C), 1431 (P–C) cm^{-1} . 1H NMR (400.13 MHz, C_6D_6 , 300 K): δ = 7.52–7.08 (m, 20H, CH arom), 2.40 (br t, 2H, CH_2 dppm), 2.19 (m, 1H, $CH-(CH_2)_3$), 1.84–1.72 (m, 6H, $CH-CH_3$), 1.45–1.34 (m, 6H, $CH_2-P^iPr_2$), 1.23–1.15 (m, 24H, $CH-CH_3$ coord.), 1.10–1.04 (m, 12H, $CH-CH_3$ uncoord.) ppm. ^{31}P NMR (161.98 MHz, C_6D_6 , 300 K) δ = 44.1 (m, 2P, P_{cb} , J = 9.5, 12.8, –25.3, 102.1 Hz), 9.5 (m, 2P, $P_{a,b}$, J = 9.5, 12.8, –25.3, 102.1 Hz), –6.1 (s, 1P, P_c) ppm.

trans-[$Mo(N_2)_2(\kappa^2-trpd-3)(dmpm)$] (6**)**. A 500 mg portion of (0.57 mmol) [$MoI_3(trpd-3)$] with 77.1 mg of (0.57 mmol) dmpm was reacted as described above. The reaction mixture was decanted and filtrated and afterward the solvent was evaporated by nitrogen steam. The achieved dark red viscous product was extracted by 20 mL of benzene which was evaporated in vacuo. Yield: 100 mg (0.144 mmol, 25%)

Anal. Calc. for $C_{27}H_{63}MoN_4P_5$: C, 46.7; H, 9.1; N, 8.1 found: C, 47.1; H, 9.2; N, 7.9.

IR (ATR): 2948–2866, 2005 (NN), 1925 (NN), 1460 (P–C), 1410 (P–C) cm^{-1} . 1H NMR (400.13 MHz, C_6D_6 , 300 K): δ = 2.37 (br t, 2H, CH_2 dmpm), 2.13 (m, 1H, $CH-(CH_2)_3$), 1.79–1.65 (m, 6H, $CH-CH_3$), 1.46–1.44 (br d, 6H, $CH_2-P^iPr_2$), 1.44–1.08 (m, 48H, 12 \times $CH-CH_3$, 4 \times CH_3 dmpm) ppm. ^{31}P NMR (161.98 MHz, C_6D_6 , 300 K) δ = 49.8 (m, 2P, P_{cb} , J = 8.4, 10.2, –26.9, 107.6 Hz), –21.75 (m, 2P, $P_{a,b}$, J = 8.4, 10.2, –26.9, 107.6 Hz), –5.7 (s, 1P, P_c) ppm.

trans-[$Mo(N_2)_2(\kappa^2-tdppmm)(dmpm)$] (7**)**. A 500 mg portion of (0.43 mmol) [$MoI_3(thf)(tdppmm)$] with 62.6 mg of (0.46 mmol) dmpm was reacted as described above. Yield: 100 mg (0.111 mmol, 26%)

Anal. Calc. for $C_{45}H_{51}MoN_4P_5$: C, 60.1; H, 5.7; N, 6.2 found: C, 59.7; H, 6.1; N, 5.9.

IR (ATR): 3033, 2955–2900, 2020 (NN), 1940 (NN), 1477 (P–C), 1430 (P–C) cm^{-1} . 1H NMR (400.13 MHz, C_6D_6 , 300 K): δ = 7.64–7.05 (m, 30H, CH arom.), 3.21 (m, 2H, CH_2 dmpm), 2.82 (br d, 4H, CH_2-PPh_2 coord.), 2.62 (d, 2H, CH_2-PPh_2 free), 2.34 (m, 1H, $CH-(CH_2)_3$), 1.12 (d, 6H, CH_3 dmpm), 0.90 (d, 6H, CH_3 dmpm) ppm. ^{31}P NMR (161.98 MHz, C_6D_6 , 300 K) δ = 44.2 (m, 2P, P_{cb} , J =

1.5, 11.5, -27.9, 110.2 Hz), -18.6 (m, 2P, P_{ab} , $J = 1.5, 11.5, -27.9, 110.2$ Hz), -22.9 (s, 1P, P_c) ppm.

[Mo(NNH₂)(trpd-1)(dmpm)](BArF)₂ (13). A 65 mg portion of (0.064 mmol) of [H(OEt)₂]₂BArF dissolved in 3 mL of CD₂Cl₂ was cooled to -10 °C and was added to 26 mg (0.032 mmol) of **1** in 3 mL of CD₂Cl₂. The light red mixture turned into dark red and was transferred into an NMR tube immediately. ¹H NMR (400.13 MHz, C₆D₆, 300 K): δ = 10.84 (br s, 1H, NNH₂), 9.43 (br s, 1H, NNH₂), 7.75 (br t, 16H, CH_o arom BArF), 7.58 (s, 8H, CH_p arom BArF), 7.56–6.83 (m, 20H, CH arom.), 3.75–3.67 (m, 2H, CH₂ dmpm), 3.50 (q, 16H, O(-CH₂-CH₃)₂ BArF), 2.52 (br t, 1H, CH-CH₃), 2.52–2.35 (m, 2H, CH₂-PPh₂), 2.20 (d, 3H, CH₃ dmpm), 1.89 (m, 2H, CH₂-PPh₂), 1.84 (d, 3H, CH₃ dmpm), 1.74 (m, 2H, CH₂-PPh₂), 1.47 (m, 1H, CH-CH₃), 1.51 (d, 3H, CH₃ dmpm), 1.29 (m, 3H, C_q-CH₃), 1.18 (t, 24H, O(-CH₂-CH₃)₂ BArF), 1.13–0.98 (m, 12H, CHCH₃), 0.56 (d, 3H, CH₃ dmpm) ppm. ³¹P NMR (161.98 MHz, CD₂Cl₂, 300 K) δ = 35.2 (dddd, 1P, P_d , $J = -18.6, -26.8, -26.5, 74.6$ Hz), 24.5 (dddd, 1P, P_e , $J = -18.6, -23.3, -34.6, 85.8$ Hz), -6.53 (dddd, 1P, P_f , $J = -26.5, -26.7, -34.6, -35.9$ Hz), -28.9 (ddd, 1P, P_g , $J = -26.7, -26.8, 85.8$ Hz), -32.2 (ddd, 1P, P_h , $J = -23.3, -35.9, 74.4$ Hz) ppm.

■ ASSOCIATED CONTENT

■ Supporting Information

Additional DTA-TG Data (Figures S1–S4), ³¹P NMR Spectra (Figures S5–S6, S12–S15), detailed coupling constant values of all ³¹P NMR spectra (Table S1), and IR/Raman spectra (Figures S7–S11). The results of DFT geometry optimizations (Cartesian coordinates) for the complexes **1**, **13** and [Mo(NNH₂)(tdppme)(dmpm)]²⁺ are given in Tables S2–S5. This material is available free of charge via the Internet at <http://pubs.acs.org>.

■ AUTHOR INFORMATION

Corresponding Author

*E-mail: ftuczek@ac.uni-kiel.de. Tel: ++49 (0)431 880 1410. Fax: ++49 (0)431 880 1520.

Notes

The authors declare no competing financial interest.

■ ACKNOWLEDGMENTS

F.T. thanks CAU Kiel for support of this research.

■ REFERENCES

- MacKay, B. A.; Fryzuk, M. D. *Chem. Rev.* **2004**, *104*, 385–401.
- Yandulov, D. V.; Schrock, R. R. *Science* **2003**, *301*, 76–78.
- Arashiba, K.; Miyake, Y.; Nishibayashi, Y. *Nat. Chem.* **2011**, *3*, 120–125.
- Pool, J. A.; Lobkovsky, E.; Chirik, P. J. *Nature* **2004**, *427*, 527–530.
- Rodriguez, M. M.; Bill, E.; Brennessel, W. W.; Holland, P. L. *Science* **2011**, *334*, 780–783.
- Takaoka, A.; Mankad, N. P.; Peters, J. C. *J. Am. Chem. Soc.* **2011**, *133*, 8440–3.
- Hinrichsen, S.; Broda, H.; Gradert, C.; Söncksen, L.; Tuzcek, F. *Annu. Rep. Prog. Chem., Sect. A: Inorg. Chem.* **2012**, *108*, 17–47.
- Pickett, C. J. *J. Biol. Inorg. Chem.* **1996**, *1*, 601–606.
- Broda, H.; Hinrichsen, S.; Tuzcek, F. *Coord. Chem. Rev.* **2013**, *257*, 587–598.
- Dreher, A.; Stephan, G.; Tuzcek, F. *Adv. Inorg. Chem.* **2009**, *61*, 367–405.
- Römer, R.; Stephan, G.; Habeck, C.; Hoberg, C.; Peters, G.; Näther, C.; Tuzcek, F. *Eur. J. Inorg. Chem.* **2008**, *2008*, 3258–3263.
- Römer, R.; Gradert, C.; Bannwarth, A.; Peters, G.; Näther, C.; Tuzcek, F. *Dalton Trans.* **2011**, *40*, 3229–3236.

(13) Söncksen, L.; Römer, R.; Näther, C.; Peters, G.; Tuzcek, F. *Inorg. Chim. Acta* **2011**, *374*, 472–479.

- Lehnert, N.; Tuzcek, F. *Inorg. Chem.* **1999**, *38*, 1659–1670.
- Lehnert, N.; Tuzcek, F. *Inorg. Chem.* **1999**, *38*, 1671–1682.
- Horn, K. H.; Lehnert, N.; Tuzcek, F. *Inorg. Chem.* **2003**, *42*, 1076–1086.
- Horn, K. H.; Böres, N.; Lehnert, N.; Mersmann, K.; Näther, C.; Peters, G.; Tuzcek, F. *Inorg. Chem.* **2005**, *44*, 3016–3030.
- Mersmann, K.; Horn, K. H.; Böres, N.; Lehnert, N.; Studt, F.; Paulat, F.; Peters, G.; Ivanovic-Burmazovic, I.; van Eldik, R.; Tuzcek, F. *Inorg. Chem.* **2005**, *44*, 3031–3045.
- Mersmann, K.; Hauser, A.; Lehnert, N.; Tuzcek, F. *Inorg. Chem.* **2006**, *45*, 5044–5056.
- Dreher, A.; Mersmann, K.; Näther, C.; Ivanovic-Burmazovic, I.; van Eldik, R.; Tuzcek, F. *Inorg. Chem.* **2009**, *48*, 2078–2093.
- Dreher, A.; Meyer, S.; Näther, C.; Westphal, A.; Broda, H.; Sarkar, B.; Kaim, W.; Kurz, P.; Tuzcek, F. *Inorg. Chem.* **2013**, *52*, 2335–2352.
- Stephan, G. C.; Sivasankar, C.; Studt, F.; Tuzcek, F. *Chem.—Eur. J.* **2008**, *14*, 644–652.
- George, T. A.; Tisdale, R. C. *J. Am. Chem. Soc.* **1985**, *107*, 5157–5159.
- George, T. A.; Tisdale, R. C. *Inorg. Chem.* **1988**, *27*, 2909–2912.
- George, T. A.; Ma, L.; Shailh, S. N.; Tisdale, R. C.; Zubieta, J. *Inorg. Chem.* **1990**, *29*, 4789–4796.
- Stephan, G. C.; Peters, G.; Lehnert, N.; Habeck, C. M.; Näther, C.; Tuzcek, F. *Can. J. Chem.* **2005**, *83*, 385–402.
- Klatt, K.; Stephan, G.; Peters, G.; Tuzcek, F. *Inorg. Chem.* **2008**, *47*, 6541–6550.
- Krahmer, J.; Broda, H.; Peters, G.; Näther, C.; Thimm, W.; Tuzcek, F. *Eur. J. Inorg. Chem.* **2011**, *2011*, 4377–4386.
- Janssen, B. C.; Asam, A.; Huttner, G.; Sernau, V.; Zsolnai, L. *Chem. Ber.* **1994**, *127*, 501–506.
- Muth, A.; Walter, O.; Huttner, G.; Asam, A.; Zsolnai, L.; Emmerich, C. *J. Organomet. Chem.* **1994**, *468*, 149–163.
- Pietsch, B.; Dahlenburg, L. *Inorg. Chim. Acta* **1988**, *145*, 195–203.
- Owens, B. E.; Poli, R.; Rheingold, A. L. *Inorg. Chem.* **1989**, *28*, 1456–1462.
- Walter, O.; Huttner, G.; Zsolnai, L. *Z. Naturforsch. B* **1993**, *48*, 636–640.
- George, T. A.; Kovar, R. A. *Inorg. Chem.* **1981**, *20*, 285–287.
- Hofacker, P.; Friebel, C.; Dehnicke, K.; Bauml, P.; Hiller, W.; Strähle, J. *Z. Naturforsch. B* **1989**, *44*, 1161–1166.
- Cotton, F. A.; Poli, R. *Inorg. Chem.* **1987**, *26*, 1514–1518.
- Calderazzo, F.; Maichle-Mössmer, C.; Pampaloni, G.; Strähle, J. *J. Chem. Soc., Dalton Trans.* **1993**, 655–658.
- Poli, R.; Krueger, S. T.; Mattamana, S. P. *Inorg. Synth.* **1998**, *32*, 198–203.
- Ishino, H.; Kuwata, S.; Ishii, Y.; Hidai, M. *Organometallics* **2001**, *20*, 13–15.
- Holleman, A. F.; Wiberg, E. *Lehrbuch der anorganischen Chemie*, 102nd ed.; Walter de Gruyter: Berlin, Germany, 2007; p 1776.
- Weiss, C. J.; Groves, A. N.; Mock, M. T.; Dougherty, W. G.; Kassel, W. S.; Helm, M. L.; DuBois, D. L.; Bullock, R. M. *Dalton Trans.* **2012**, *41*, 4517–4529.
- Holland, P. L. *Dalton Trans.* **2010**, *39*, 5415–5425.
- Studt, F.; Tuzcek, F. *J. Comput. Chem.* **2006**, *27*, 1278–1291.
- Tuzcek, F.; Horn, K. H.; Lehnert, N. *Coord. Chem. Rev.* **2003**, *245*, 107–120.
- Ugi, I.; Marquard, D.; Klusacek, H.; Gillespi, P.; Ramirez, F. *Acc. Chem. Res.* **1971**, *4*, 288–296.
- Günther, H. *Angew. Chem., Int. Ed.* **1972**, *11*, 861–920.
- Brookhart, M.; Grant, B.; Volpe, A. F. *Organometallics* **1992**, *11*, 3920–3922.
- Lehnert, N.; Wiesler, B. E.; Tuzcek, F.; Hennige, A.; Sellmann, D. *J. Am. Chem. Soc.* **1997**, *119*, 8879–8888.
- Tolman, C. A. *Chem. Rev.* **1977**, *77*, 313–348.

(50) No examples for a $[\text{MoP}_5]$ complex could be found in the Cambridge Structural Database (CSD).

(51) Friesen, D. M.; Bowles, O. J.; McDonald, R.; Rosenberg, L. *Dalton Trans.* **2006**, 2671–2682.

(52) Burk, M. J.; Harlow, R. L. *Angew. Chem., Int. Ed.* **1990**, *29*, 1462–1464.

(53) Latour, S.; Wuest, J. D. *Synthesis* **1987**, 742–745.

(54) Fieser, L. F.; Fieser, M. *Reagents for Organic Synthesis*; Wiley & Sons: New York, 1967; Vol. 1, p 584.

(55) Zhu, K. M.; Achord, P. D.; Zhang, X. W.; Krogh-Jespersen, K.; Goldman, A. S. *J. Am. Chem. Soc.* **2004**, *126*, 13044–13053.

(56) Naghypour, A.; Sabounchei, S. J.; Morales-Morales, D.; Hernandez-Ortega, S.; Jensen, C. M. *J. Organomet. Chem.* **2004**, *689*, 2494–2502.

(57) Stoffelbach, F.; Saurenz, D.; Poli, R. *Eur. J. Inorg. Chem.* **2001**, 2699–2703.

(58) Reger, D. L.; Wright, T. D.; Little, C. A.; Lamba, J. J. S.; Smith, M. D. *Inorg. Chem.* **2001**, *40*, 3810–3814.

(59) Hughes, R. P.; Lindner, D. C.; Rheingold, A. L.; Yap, G. P. A. *Inorg. Chem.* **1997**, *36*, 1726–1727.

(60) Frisch, M. J.; Trucks, G. W.; Schlegel, H. B.; Scuseria, G. E.; Robb, M. A.; Cheeseman, J. R.; Scalmani, G.; Barone, V.; Mennucci, B.; Petersson, G. A.; Nakatsuji, H.; Caricato, M.; Li, X.; Hratchian, H. P.; Izmaylov, A. F.; Bloino, J.; Zheng, G.; Sonnenberg, J. L.; Hada, M.; Ehara, M.; Toyota, K.; Fukuda, R.; Hasegawa, J.; Ishida, M.; Nakajima, T.; Honda, Y.; Kitao, O.; Nakai, H.; Vreven, T.; Montgomery, J., J. A.; Peralta, J. E.; Ogliaro, F.; Bearpark, M.; Heyd, J. J.; Brothers, E.; Kudin, K. N.; Staroverov, V. N.; Kobayashi, R.; Normand, J.; Raghavachari, K.; Rendell, A.; Burant, J. C.; Iyengar, S. S.; Tomasi, J.; Cossi, M.; Rega, N.; Millam, J. M.; Klene, M.; Knox, J. E.; Cross, J. B.; Bakken, V.; Adamo, C.; Jaramillo, J.; Gomperts, R.; Stratmann, R. E.; Yazyev, O.; Austin, A. J.; Cammi, R.; Pomelli, C.; Ochterski, J. W.; Martin, R. L.; Morokuma, K.; Zakrzewski, V. G.; Voth, G. A.; Salvador, P.; Dannenberg, J. J.; Dapprich, S.; Daniels, A. D.; Farkas, Ö.; Foresman, J. B.; Ortiz, J. V.; Cioslowski, J.; Fox, D. J. *Gaussian 09*, Revision A.02; Gaussian, Inc.: Wallingford, CT, 2009.

(61) Sheldrick, G. M. *Acta Crystallogr.* **2008**, *64*, 112–122.

(62) *X-Area, Program Package for Single Crystal Measurements*, Version 1.44; STOE & CIE GmbH: Darmstadt, Germany, 2008.

(63) Spek, A. L. *J. Appl. Crystallogr.* **2003**, *36*, 7–13.